JHEP

Published for SISSA by Springer

Received: July 22, 2016
Revised: September 14, 2016
Accepted: September 15, 2016
Published: September 21, 2016

On a radiative origin of the Standard Model from trinification

José Eliel Camargo-Molina,[a] **António P. Morais,**[a,b] **Roman Pasechnik**[a] **and Jonas Wessén**[a]

[a] *Department of Astronomy and Theoretical Physics, Lund University, Sölvegatan 14A, SE-223 62 Lund, Sweden*

[b] *Departamento de Física, Universidade de Aveiro and CIDMA, Campus de Santiago, 3810-183 Aveiro, Portugal*

E-mail: Eliel@thep.lu.se, Aapmorais@ua.pt, Roman.Pasechnik@thep.lu.se, Jonas.Wessen@thep.lu.se

Abstract: In this work, we present a trinification-based grand unified theory incorporating a global SU(3) family symmetry that after a spontaneous breaking leads to a left-right symmetric model. Already at the classical level, this model can accommodate the matter content and the quark Cabbibo mixing in the Standard Model (SM) with only one Yukawa coupling at the unification scale. Considering the minimal low-energy scenario with the least amount of light states, we show that the resulting effective theory enables dynamical breaking of its gauge group down to that of the SM by means of radiative corrections accounted for by the renormalisation group evolution at one loop. This result paves the way for a consistent explanation of the SM breaking scale and fermion mass hierarchies.

Keywords: GUT, Effective field theories, Spontaneous Symmetry Breaking, Renormalization Group

ArXiv ePrint: 1606.03492

doi:10.1007/JHEP09(2016)129

JHEP09(2016)129

Contents

JHEP09(2016)129

1 Introduction

The discovery of the Higgs boson at the Large Hadron Collider (LHC) [1, 2] and continuous studies of its properties have revealed an intriguing consistency of experimental results with the Standard Model (SM) predictions. This highlights yet another major step in precision verification of the SM structure. Besides being a big phenomenological success as a fundamental theory of particle physics, the SM as an effective theory still allows for possibilities for new interactions and particles (such as Dark Matter, right-handed neutrinos, heavy Higgs boson partners, new gauge interactions, among others) at energy scales much larger then the electroweak (EW) scale. This kind of new physics might bring answers to current open questions and could be detected already at the LHC. In addition, the origin of the large set of measured (not predicted!) fermion mass and mixing parameters as well as the Higgs boson mass and self-couplings still remains as one of the most interesting open questions to date. Furthermore, there is still no explanation for the characteristic hierarchies in the measured fermion mass spectrum.

In order to get a better understanding of these long-standing issues in the framework of quantum field theory, one naturally considers the SM as a low-energy approximation of a bigger and more symmetric (unified) theory whose dynamics at high energies is implicitly encoded in the observed structure of the SM.

An important example of such a grand unified theory (GUT) based upon the trinified gauge group $\mathrm{SU}(3)_\mathrm{L} \times \mathrm{SU}(3)_\mathrm{R} \times \mathrm{SU}(3)_\mathrm{C} \equiv [\mathrm{SU}(3)]^3$ (also known as trinification) was proposed by De Rújula, Georgi and Glashow (RGG-model) back in 1984 [3]. Since then, trinified extensions of the SM have been traditionally considered as good bets for a GUT, both with and without supersymmetry (SUSY) [4–9], due to many attractive features (for a good introduction into trinification GUTs, see [10] and references therein).

The gauge trinification $[\mathrm{SU}(3)]^3 \ltimes \mathbb{Z}_3$ is a maximal subgroup of E_6, where $\mathbb{Z}_3$ is the group of cyclic (L,R,C)-permutations (for a comprehensive discussion of E_6-inspired GUT scenarios, see e.g. refs. [11–37]). Typically, this model is considered to be a low-energy limit of the heteroic $\mathrm{E}_8 \times \mathrm{E}_8'$ string theory [38] as well as the $\mathcal{N} = 4$ supergravity [39]. It naturally incorporates the left-right (LR) symmetric gauge interactions [40] as well as the gauge couplings' unification at a GUT scale. All matter fields (including the Higgs fields) can be elegantly arranged into bi-fundamental representations where each family belongs to a **27**-plet, $\mathbf{27} = (\mathbf{3}, \bar{\mathbf{3}}, \mathbf{1}) \oplus (\mathbf{1}, \mathbf{3}, \bar{\mathbf{3}}) \oplus (\bar{\mathbf{3}}, \mathbf{1}, \mathbf{3})$, being the fundamental representation of the E_6 group [11, 41]. Remarkably, no adjoint Higgs fields are needed to break $\mathrm{SU}(3)_\mathrm{L} \times$

JHEP09(2016)129

$SU(3)_R$ down to the electroweak (EW) symmetry group of the SM, $SU(2)_L \times U(1)_Y$. The spontaneous breaking of trinification with at least two Higgs **27**-plets yields the standard GUT-scale prediction for the weak mixing angle, $\sin^2\theta_W = 3/8$, which leads to quantization of the $U(1)_Y$ hypercharge in the SM (e.g. resulting in electron charge being exactly opposite to the proton charge) and provides a consistent explanation of parity violation in the SM. As was shown in refs. [42, 43] it is possible to achieve naturally light neutrinos via a seesaw mechanism as well. Moreover, in the RGG formulation, the model accommodates any quark mixing angles [44] and a natural suppression of proton decay [4, 8].

However, many existing realizations of the RGG model suffer from severe issues with phenomenology, a considerable amount of particles in its spectrum and many (e.g. Yukawa) parameters. One particular issue, common to most of the well-known GUTs, is an unmotivated strong hierarchy between the trinification and the EW symmetry breaking scales as well as hierarchies in the SM fermion mass spectrum. In addition, the existing minimal SUSY-based trinification [44] has problems in avoiding TeV-scale lepton masses without imposing higher-dimensional operators, large Higgs representations or an artificial and simultaneous fine tuning of many parameters. At the same time, realistic calculations including quantum corrections are cumbersome due to a large number of scalar particles and gauge bosons in any $[SU(3)]^3$-symmetric theory. These issues left the trinification-based models among the least-developed GUT scenarios so far.

To be consistent with SM phenomenology, a number of additional U(1) groups emerging in E_6 (or E_8) breaking [45] should be consistently broken at intermediate steps by the conventional Higgs mechanism. Having a few **27** Higgs multiplets coupled to fermions which acquire several low-scale vacuum expectation values (VEVs), may resolve this issue. However, those interactions induce potentially large flavour-changing neutral current processes which are severely restricted by experiment, and a large degree of fine tuning is required.

Due to a huge hierarchy in the mass spectra, at low energy scales heavy d.o.f.'s have to be integrated out at each intermediate symmetry breaking scale giving rise to a new effective model having a fewer amount of light fields in the spectrum. Depending on the symmetry breaking scheme and the hierarchy in the initial $[SU(3)]^3$ GUT model parameters, one may end up with a few possible low-energy effective models having different light particle content.

One possible development would be to consider a mechanism for Yukawa couplings unification, severely reducing the number of free parameters at the GUT scale [15, 16]. Similarly to the gauge couplings, the unified Yukawa coupling would then give rise to several different couplings by means of radiative corrections via the renormalisation group (RG) evolution and loop-induced operators, which may reproduce the SM fermion mass and mixing hierarchies at low energies. In this way, family symmetries acting in the space of fermion generations [46] are known to provide a convenient tool for generating the necessary patterns in fermion spectra [16, 47]. In particular, such symmetries help to avoid GUT-scale lepton masses in trinification-type models.

An example of an effective LR-symmetric scenario with very interesting phenomenology has been discussed in ref. [48]. There the authors introduce the gauge group $SU(3)_C \times SU(2)_L \times SU(2)_R \times U(1)_{B-L}$ as originating at lower energies from the trinification model with

JHEP09(2016)129

two $\mathbb{Z}_2$-even and odd Higgs **27**-plets. However, the properties of the Yukawa sector in this model rely on additional higher-dimensional representations of E_6 such as (anti)symmetric **351** reps.

In this work, we consider an alternative non-SUSY trinification model $[SU(3)]^3 \ltimes \mathbb{Z}_3$ augmented by a $SU(3)_F$ global family symmetry which acts both on fermion and scalar multiplets. The latter are thus incorporated in a symmetric way essentially inspired by SUSY. Our scenario is however manifestly non-supersymmetric and it does not invoke any higher-dimensional reps or extra singlets besides lowest **27**-plets of E_6. The scenario we present is naturally inspired by a reduction $E_8 \to E_6 \times SU(3)$ where the remnant $SU(3)$ is identified with a global family symmetry $SU(3)_F$ at the trinification breaking scale. The symmetry group is spontaneously broken down to a LR-symmetric model with an extra $SU(2)_F \times U(1)_X \times U(1)_Z \times U(1)_B$ global symmetry that is a remnant of the $SU(3)_F$ and an accidental $U(1)_A \times U(1)_B$ symmetry in the high-scale trinification theory.

As we show in the present work, this model inherits all the important features of trinified GUTs and resolves some of their known difficulties. In the considered implementation of the family symmetry together with the trinification model, all Yukawa couplings are manifestly unified into a single coupling at the GUT scale, and the number of free scalar self-couplings in the scalar potential is remarkably low, making a complete RG analysis of this model feasible. Many of the relevant interactions in the low-energy effective theory emerge radiatively at one (or higher) loop level, bringing a potential explanation to a variety of hierarchies in the SM parameters. However, a detailed calculation of such quantities is beyond the scope of this paper and left for future work. Simultaneously, the family symmetry forbids proton decay due to an appearance of an accidental $U(1)_B$ symmetry and protects the light SM fermion sector from large radiative corrections offering potentially interesting phenomenological consequences. Another feature of this model, that we show in this work, is that the $SU(2)_R \times U(1)_{L+R}$ subgroup gets broken radiatively to $U(1)_Y$ at a much lower scale in a natural way for a large region of the parameter space of the GUT-scale trinification model.

In section 2, we introduce the high-scale trinification model augmented by the family symmetry. In section 3, we discuss in detail the first symmetry breaking stage down to a low-energy LR-symmetric effective theory. In section 4, we describe the effective model and the matching of effective couplings in order to study, in section 5, under which circumstances the effective theory shows radiative breaking of the $SU(2)_R \times U(1)_{L+R}$ symmetry. In section 6, we perform a parameter space scan to find the regions where the radiative symmetry breaking happens in the simplest feasible scenario. In section 7 we discuss, in the light of our results, under which conditions it could be possible to reproduce the SM mass spectra. Concluding remarks are given in section 8.

1.1 A quick note on notations

In the text that follows, we employ the following notations:

- Fundamental representations carry superscript indices while anti-fundamental representations carry subscript indices.

JHEP09(2016)129

- Fundamental and anti-fundamental indices of SU(3) groups are denoted with lower case letters, while fundamental and anti-fundamental indices under SU(2) groups are denoted with upper case letters.
- $\mathrm{SU}(3)_\mathrm{K}$ and $\mathrm{SU}(2)_\mathrm{K}$ (anti-)fundamental indices are denoted by $k, k', k_1, k_2 \ldots$ and $K, K', K_1, K_2 \ldots$ for $K = L, R, C$, respectively.
- Indices belonging to (anti-)fundamental representations of $\mathrm{SU}(3)_\mathrm{F}$ and $\mathrm{SU}(2)_\mathrm{F}$ are denoted by $i, j, k \ldots$ and $I, J, K \ldots$ respectively.
- If a field transforms both under gauge and global symmetry groups, the index corresponding to the global one is placed within the parenthesis around the field, while the indices corresponding to the gauge symmetries are placed outside.
- Global symmetry groups will be indicated by $\{\ldots\}$.

For example, $(L^i)^l_r$ is a $\mathbf{3}\otimes\mathbf{3}\otimes\bar{\mathbf{3}}$ representation of $\mathrm{SU}(3)_\mathrm{L}\times\mathrm{SU}(3)_\mathrm{R}\times\{\mathrm{SU}(3)_\mathrm{F}\}$, and $(\tilde{l}_\mathrm{R}{}^I)_R$ is a $\mathbf{2}\otimes\bar{\mathbf{2}}$ representation of $\mathrm{SU}(2)_\mathrm{R}\times\{\mathrm{SU}(2)_\mathrm{F}\}$, where $\mathrm{SU}(3)_\mathrm{F}$ and $\mathrm{SU}(2)_\mathrm{F}$ are global family symmetry groups.

2 The GUT-scale $[\mathrm{SU}(3)]^3 \ltimes \mathbb{Z}_3 \times \{\mathrm{SU}(3)_\mathrm{F}\}$ model

The fields in the high-scale trinification model form representations of the symmetry group

$$[\mathrm{SU}(3)_\mathrm{L}\times\mathrm{SU}(3)_\mathrm{R}\times\mathrm{SU}(3)_\mathrm{C}]\ltimes\mathbb{Z}_3\times\{\mathrm{SU}(3)_\mathrm{F}\}, \tag{2.1}$$

as shown in table 1, and consist of three Weyl fermion multiplets (L, Q_L, Q_R), three scalar multiplets ($\tilde{L}$, $\tilde{Q}_\mathrm{L}$, $\tilde{Q}_\mathrm{R}$) and gauge bosons (G_L, G_R, G_C). Here, $\mathrm{SU}(3)_\mathrm{F}$ is a global family symmetry acting on the space of fermion and scalar field generations, while $\mathrm{SU}(3)_\mathrm{L}\times\mathrm{SU}(3)_\mathrm{R}\times\mathrm{SU}(3)_\mathrm{C}$ is the standard trinification gauge group. Although our model is not supersymmetric, we employ a notation inspired by SUSY, since we have the same group representations in the scalar and fermion sectors. The fermions and scalars both form bi-triplet representations under the gauge group, but *tri*-triplets under the full symmetry group (including the $\mathrm{SU}(3)_\mathrm{F}$).[1]

The $\mathbb{Z}_3$ symmetry refers to the cyclic permutation of the fields

$$\begin{aligned}
&G_\mathrm{L}\overset{\mathbb{Z}_3}{\to}G_\mathrm{C}, && L\overset{\mathbb{Z}_3}{\to}Q_\mathrm{L}, && \tilde{L}\overset{\mathbb{Z}_3}{\to}\tilde{Q}_\mathrm{L},\\
&G_\mathrm{C}\overset{\mathbb{Z}_3}{\to}G_\mathrm{R}, && Q_\mathrm{L}\overset{\mathbb{Z}_3}{\to}Q_\mathrm{R}, && \tilde{Q}_\mathrm{L}\overset{\mathbb{Z}_3}{\to}\tilde{Q}_\mathrm{R},\\
&G_\mathrm{R}\overset{\mathbb{Z}_3}{\to}G_\mathrm{L}, && Q_\mathrm{R}\overset{\mathbb{Z}_3}{\to}L, && \tilde{Q}_\mathrm{R}\overset{\mathbb{Z}_3}{\to}\tilde{L}.
\end{aligned} \tag{2.2}$$

which in turn enforces the gauge coupling unification. This symmetry combined with the global $\mathrm{SU}(3)_\mathrm{F}$ also dramatically reduces the number of possible terms in the scalar potential as well as in the fermion sector of the theory.

[1] Gauging the family $\mathrm{SU}(3)_\mathrm{F}$ in an E_8 inspired scenario would effectively mean the doubling the number of chiral and scalar multiplets as is required by the anomaly cancellation condition. In this paper, however, we avoid such a huge complication by treating the family symmetry as a global one, as a first step.

JHEP09(2016)129

	$\mathrm{SU}(3)_\mathrm{L}$	$\mathrm{SU}(3)_\mathrm{R}$	$\mathrm{SU}(3)_\mathrm{C}$	$\{\mathrm{SU}(3)_\mathrm{F}\}$
fermions				
L	$\mathbf{3}$	$\bar{\mathbf{3}}$	$\mathbf{1}$	$\mathbf{3}$
Q_L	$\bar{\mathbf{3}}$	$\mathbf{1}$	$\mathbf{3}$	$\mathbf{3}$
Q_R	$\mathbf{1}$	$\mathbf{3}$	$\bar{\mathbf{3}}$	$\mathbf{3}$
scalars				
$\tilde{L}$	$\mathbf{3}$	$\bar{\mathbf{3}}$	$\mathbf{1}$	$\mathbf{3}$
$\tilde{Q}_\mathrm{L}$	$\bar{\mathbf{3}}$	$\mathbf{1}$	$\mathbf{3}$	$\mathbf{3}$
$\tilde{Q}_\mathrm{R}$	$\mathbf{1}$	$\mathbf{3}$	$\bar{\mathbf{3}}$	$\mathbf{3}$
gauge bosons				
G_L	$\mathbf{8}$	$\mathbf{1}$	$\mathbf{1}$	$\mathbf{1}$
G_R	$\mathbf{1}$	$\mathbf{8}$	$\mathbf{1}$	$\mathbf{1}$
G_C	$\mathbf{1}$	$\mathbf{1}$	$\mathbf{8}$	$\mathbf{1}$

Table 1. Field content of the GUT-scale trinification model. The fermionic fields are left-handed Weyl fermions.

The most general renormalizable scalar potential for the trinification model reads

$$V = V_1 + V_2 + V_3 \tag{2.3}$$

where

$$\begin{aligned} V_1 = {} & -\mu^2 (\tilde{L}^i)^l_r \, (\tilde{L}^*_i)^r_l + \lambda_1 \left[(\tilde{L}^i)^l_r \, (\tilde{L}^*_i)^r_l \right]^2 + \lambda_2 (\tilde{L}^i)^l_r \, (\tilde{L}^j)^{l'}_{r'} \, (\tilde{L}^*_j)^r_l \, (\tilde{L}^*_i)^{r'}_{l'} \\ & + \lambda_3 (\tilde{L}^i)^l_r \, (\tilde{L}^j)^{l'}_{r'} \, (\tilde{L}^*_i)^{r'}_l \, (\tilde{L}^*_j)^r_{l'} + \lambda_4 \, (\tilde{L}^i)^l_r \, (\tilde{L}^j)^{l'}_{r'} \, (\tilde{L}^*_j)^{r'}_l \, (\tilde{L}^*_i)^r_{l'} \\ & + (\mathbb{Z}_3 \text{ permutations}), \\ V_2 = {} & \alpha_1 \, (\tilde{L}^i)^l_r \, (\tilde{L}^*_i)^r_l \, (\tilde{Q}_\mathrm{L}{}^j)^c_{l'} \, (\tilde{Q}^*_{\mathrm{L}j})^{l'}_c + \alpha_2 \, (\tilde{L}^i)^l_r \, (\tilde{L}^*_j)^r_l \, (\tilde{Q}_\mathrm{L}{}^j)^c_{l'} \, (\tilde{Q}^*_{\mathrm{L}i})^{l'}_c \\ & + \alpha_3 \, (\tilde{L}^i)^l_r \, (\tilde{L}^*_i)^r_{l'} \, (\tilde{Q}_\mathrm{L}{}^j)^c_l \, (\tilde{Q}^*_{\mathrm{L}j})^{l'}_c + \alpha_4 \, (\tilde{L}^i)^l_r \, (\tilde{L}^*_j)^r_{l'} \, (\tilde{Q}_\mathrm{L}{}^j)^c_l \, (\tilde{Q}^*_{\mathrm{L}i})^{l'}_c \\ & + (\mathbb{Z}_3 \text{ permutations}), \end{aligned} \tag{2.4}$$

and

$$V_3 = \gamma \, \epsilon_{ijk} \, (\tilde{L}^i)^l_r \, (\tilde{Q}_\mathrm{L}{}^j)^c_l \, (\tilde{Q}_\mathrm{R}{}^k)^r_c + \text{c.c.} \tag{2.5}$$

The scalar potential thus contains two dimensionfull parameters, mass parameter μ and trilinear coupling γ, and eight quartic couplings $\lambda_{1,\ldots,4}$ and $\alpha_{1,\ldots,4}$ which can be taken to be real without loss of generality.

Due to the interplay between $\mathrm{SU}(3)_\mathrm{F}$ and $\mathbb{Z}_3$, combined with the trinification gauge group, the fermion sector in the model only contains one single Yukawa coupling,

$$\mathcal{L}_\mathrm{Fermion} = -y \, \epsilon_{ijk} \, (\tilde{L}^i)^l_r \, (Q_\mathrm{L}{}^j)^c_l \, (Q_\mathrm{R}{}^k)^r_c + \text{c.c.} + (\mathbb{Z}_3 \text{ permutations}). \tag{2.6}$$

The trinification Yukawa coupling y can be taken to be real since any complex phase may be absorbed into the definition of the fermion fields.

JHEP09(2016)129

	$\mathrm{U}(1)_\mathrm{A}$	$\mathrm{U}(1)_\mathrm{B}$
L, $\tilde{L}$	$+1$	0
Q_L, $\tilde{Q}_\mathrm{L}$	$-1/2$	$+1/3$
Q_R, $\tilde{Q}_\mathrm{R}$	$-1/2$	$-1/3$
$G_\mathrm{L,R,C}$	0	0

Table 2. Charge assignment under the accidental symmetries.

Once all the renormalizable terms invariant under the trinification gauge group and the global $\mathrm{SU}(3)_\mathrm{F}$ symmetry are written, one can notice that the terms are also invariant under an accidental $\{\mathrm{U}(1)_\mathrm{A} \times \mathrm{U}(1)_\mathrm{B}\}$ symmetry. A convenient charge assignment under the accidental U(1) groups is shown in table 2, where one immediately recognizes $\mathrm{U}(1)_\mathrm{B}$ as giving rise to a conserved baryon number. Furthermore, $\mathrm{U}(1)_\mathrm{B}$ will stay unbroken at lower scales (including the SM), since $\tilde{L}$ is uncharged under $\mathrm{U}(1)_\mathrm{B}$ and no other fields will develop VEVs throughout the evolution to the EW scale. Though the symmetry would still allow for the proton to decay into coloured scalars $\tilde{Q}_\mathrm{L,R}$, we will see that all the coloured scalar states acquire their masses of the order of the unification scale (i.e. much larger than the proton mass), making such a proton decay kinematically impossible. Meanwhile, the heavy coloured scalars are relevant for generation of loop-induced lepton mass terms at the matching scale in the low-energy effective model as will be discussed in more detail below.

3 Spontaneous trinification breaking down to a LR-symmetric model

In this paper, we would like to explore whether after the spontaneous symmetry breaking (SSB) of the trinification gauge symmetry, it will be possible for the effective LR-symmetric model to break down to the SM gauge group by means of the RG evolution of the corresponding couplings, in particular, mass parameters. In order to do that, one has to explore first the SSB of the group in eq. (2.1) (also taking into account the accidental $\{\mathrm{U}(1)_\mathrm{A} \times \mathrm{U}(1)_\mathrm{B}\}$ symmetry). The most straightforward way to break trinification is when only one component in $\tilde{L}$ acquires a real non-zero VEV, namely,

$$\langle (\tilde{L}^i)^l_r \rangle = \delta^i_3 \delta^l_3 \delta^3_r \frac{v_3}{\sqrt{2}} = \begin{pmatrix} 0 & 0 & 0 \\ 0 & 0 & 0 \\ 0 & 0 & \frac{v_3}{\sqrt{2}} \end{pmatrix}^{i=3} , \tag{3.1}$$

where the l (r) index labels the rows (columns), while $\langle \tilde{Q}_L \rangle = \langle \tilde{Q}_R \rangle = 0$. As will be shown in section 3.5, this often corresponds to the global minimum of the potential in eq. (2.3), assuming no $\mathrm{SU}(3)_\mathrm{C}$ breaking VEVs. The extremal conditions (i.e. the requirement that the first derivatives of the scalar potential vanish in the minimum) allow us to rewrite μ in terms of v_3 as follows

$$\mu^2 = (\lambda_1 + \lambda_2 + \lambda_3 + \lambda_4)\, v_3^2 \,. \tag{3.2}$$

JHEP09(2016)129

By applying a general infinitesimal gauge transformation on $\langle(\tilde{L}^i)^l_r\rangle$, we find that the following subset of the trinification gauge symmetry generators leaves that vacuum invariant:

$$T_{\rm C}^{1,\ldots,8}\,, \qquad T_{\rm L}^{1,2,3}\,, \qquad T_{\rm R}^{1,2,3}\,, \qquad T_{\rm L+R} \equiv \frac{2}{\sqrt{3}}\left(T_{\rm L}^8 + T_{\rm R}^8\right)\,. \tag{3.3}$$

Therefore, the vacuum (3.1) spontaneously breaks the trinification gauge group to the LR-symmetric gauge group $\mathrm{SU}(3)_{\rm C} \times \mathrm{SU}(2)_{\rm L} \times \mathrm{SU}(2)_{\rm R} \times \mathrm{U}(1)_{\rm L+R}$. Before the SSB, the global symmetry group is the full symmetry group $\mathrm{SU}(3)_{\rm C} \times \mathrm{SU}(3)_{\rm L} \times \mathrm{SU}(3)_{\rm R} \times \mathrm{SU}(3)_{\rm F} \times \mathrm{U}(1)_{\rm A} \times \mathrm{U}(1)_{\rm B}$. When applying a general infinitesimal global symmetry transformation on the vacuum given by eq. (3.1), we find that the following generators leave it invariant

$$T_{\rm F}^{1,2,3}\,, \qquad T_{\rm X} \equiv \frac{2}{\sqrt{3}}\left(T_{\rm L}^8 - T_{\rm R}^8 - 2T_{\rm F}^8\right)\,, \qquad T_{\rm Z} \equiv \frac{2}{3}\left(T_{\rm A} + \sqrt{3}T_{\rm F}^8\right)\,, \tag{3.4}$$

in addition to $T_{\rm B}$ and the generators in eq. (3.3). Here, we have constructed $T_{\rm X,Z}$ such that they are orthogonal to $T_{\rm L+R}$ and chosen their normalisation for convenience. However, any other two linearly independent combinations of $T_{\rm X,Z}$ and $T_{\rm L+R}$ that are also linearly independent of $T_{\rm L+R}$, generate an unbroken $\{\mathrm{U}(1)\times\mathrm{U}(1)\}$ symmetry. Therefore, after the SSB, in addition to the unbroken gauge group, the symmetry $\{\mathrm{SU}(2)_{\rm F}\times\mathrm{U}(1)_{\rm X}\times\mathrm{U}(1)_{\rm Z}\times\mathrm{U}(1)_{\rm B}\}$ remains unbroken as well. In summary, the VEV setting (3.1) leads to the SSB pattern

$$\begin{gathered}\mathrm{SU}(3)_{\rm L} \times \mathrm{SU}(3)_{\rm R} \times \mathrm{SU}(3)_{\rm C} \times \{\mathrm{SU}(3)_{\rm F} \times \mathrm{U}(1)_{\rm A} \times \mathrm{U}(1)_{\rm B}\} \\ \downarrow \\ \mathrm{SU}(3)_{\rm C} \times \mathrm{SU}(2)_{\rm L} \times \mathrm{SU}(2)_{\rm R} \times \mathrm{U}(1)_{\rm L+R} \times \{\mathrm{SU}(2)_{\rm F} \times \mathrm{U}(1)_{\rm X} \times \mathrm{U}(1)_{\rm Z} \times \mathrm{U}(1)_{\rm B}\}\,,\end{gathered} \tag{3.5}$$

and the basic properties of the resulting effective LR-symmetric model will be studied below in detail.

3.1 Colour-singlet scalar sector

The colour-singlet scalars (CSS) are contained in $\tilde{L}$ which is the tri-triplet representation $\mathbf{3}\otimes\bar{\mathbf{3}}\otimes\mathbf{3}$ of $\mathrm{SU}(3)_{\rm L}\times\mathrm{SU}(3)_{\rm R}\times\{\mathrm{SU}(3)_{\rm F}\}$. It therefore contains 54 real degrees of freedom. The VEV structure (3.1) breaks nine gauge symmetry generators, meaning that one identifies nine massless real d.o.f.'s in the CSS mass spectrum that become the longitudinal polarisation states of nine massive gauge bosons. In addition, the non-gauge part of the symmetry group is reduced from $\mathrm{SU}(3)_{\rm F}\times\mathrm{U}(1)_{\rm A}\times\mathrm{U}(1)_{\rm B}$ down to $\mathrm{SU}(2)_{\rm F}\times\mathrm{U}(1)_{\rm X}\times\mathrm{U}(1)_{\rm Z}\times\mathrm{U}(1)_{\rm B}$ so that the CSS spectrum, after the SSB, also contains four corresponding Goldstone d.o.f.'s. These so-called "global Goldstone" bosons remain as physical massless scalar d.o.f.'s. However, at energy scales much lower than v_3, these are effectively decoupled from all other light fields (including the SM fields) since their interactions are always suppressed by powers of v_3. The decoupling of global Goldstone bosons is further discussed in section 4.4. The mass eigenstates and the corresponding squared masses of the CSS after $(\tilde{L}^3)^3_3$ develops a VEV, are listed in table 3. Local stability of the minima in the CSS sector is obtained when these squared masses are non-negative. Combined with the requirement that $\mu^2 > 0$, this is ensured when

$$\lambda_1+\lambda_2+\lambda_3+\lambda_4 > 0\,, \qquad \lambda_2+\lambda_3 \leq 0\,, \qquad \lambda_2+\lambda_4 \leq 0\,, \qquad \lambda_3+\lambda_4 \leq 0\,. \tag{3.6}$$

JHEP09(2016)129

Fields	$(\text{Mass})^2$	$(L+R, X, Z)$	Comment
$(\tilde{L}^I)^L_R$	$-(\lambda_2+\lambda_3+\lambda_4)\,v_3^2$	$(0,0,+1)$	
$(\tilde{L}^I)^3_R$	$m_R^2 \equiv -(\lambda_2+\lambda_3)\,v_3^2$	$(-1,-1,+1)$	
$(\tilde{L}^3)^L_R$	$m_h^2 \equiv -(\lambda_3+\lambda_4)\,v_3^2$	$(0,+2,0)$	
$(\tilde{L}^I)^L_3$	$-(\lambda_2+\lambda_4)\,v_3^2$	$(+1,-1,+1)$	
$\text{Re}[(\tilde{L}^3)^3_3]$	$2(\lambda_1+\lambda_2+\lambda_3+\lambda_4)\,v_3^2$	$(0,0,0)$	
$\text{Im}[(\tilde{L}^3)^3_3]$	0	$(0,0,0)$	Gauge Goldstone
$(\tilde{L}^3)^L_3$	0	$(+1,+1,0)$	Gauge Goldstone
$(\tilde{L}^3)^3_R$	0	$(-1,+1,0)$	Gauge Goldstone
$(\tilde{L}^I)^3_3$	0	$(0,-2,+1)$	Global Goldstone

Table 3. Mass eigenstates in $\tilde{L}$ after the SSB of the trinification group, and the corresponding tree-level squared masses and U(1) charges. All states have zero baryon number here. In section 4, we consider the LR-symmetric low-energy effective model with $(\tilde{L}^I)^3_R \equiv (\tilde{l}_{\rm R}{}^I)_R$ and $(\tilde{L}^3)^L_R \equiv \tilde{h}^L_R$ assuming that $m^2_{R,h} \ll v_3^2$ while all other masses are heavy, i.e. $\sim v_3$.

Fields	$(\text{Mass})^2$	$(L+R, X, Z, B)$
$(\tilde{Q}_{\rm L}{}^I)^c_L$	$\frac{1}{2}\left[\alpha_1 - 2(\lambda_1+\lambda_2+\lambda_3+\lambda_4)\right] v_3^2$	$(-1/3,-1,0,+1/3)$
$(\tilde{Q}_{\rm R}{}^I)^R_c$	$\frac{1}{2}\left[\alpha_1 - 2(\lambda_1+\lambda_2+\lambda_3+\lambda_4)\right] v_3^2$	$(+1/3,-1,0,-1/3)$
$(\tilde{Q}_{\rm L}{}^3)^c_L$	$\frac{1}{2}\left[\alpha_1+\alpha_2 - 2(\lambda_1+\lambda_2+\lambda_3+\lambda_4)\right] v_3^2$	$(-1/3,+1,-1,+1/3)$
$(\tilde{Q}_{\rm R}{}^3)^R_c$	$\frac{1}{2}\left[\alpha_1+\alpha_2 - 2(\lambda_1+\lambda_2+\lambda_3+\lambda_4)\right] v_3^2$	$(+1/3,+1,-1,-1/3)$
$(\tilde{Q}^I_{\rm LR\pm})^c$	$\frac{1}{2}\left[\alpha_1+\alpha_3 \pm \frac{\gamma}{\sqrt{2}v_3} - 2(\lambda_1+\lambda_2+\lambda_3+\lambda_4)\right] v_3^2$	$(+2/3,0,+1/3)$
$(\tilde{Q}_{\rm L}{}^3)^c_3$	$\frac{1}{2}\left[\alpha_1+\alpha_2+\alpha_3+\alpha_4 - 2(\lambda_1+\lambda_2+\lambda_3+\lambda_4)\right] v_3^2$	$(+2/3,+2,-1,+1/3)$
$(\tilde{Q}_{\rm R}{}^3)^3_c$	$\frac{1}{2}\left[\alpha_1+\alpha_2+\alpha_3+\alpha_4 - 2(\lambda_1+\lambda_2+\lambda_3+\lambda_4)\right] v_3^2$	$(-2/3,+2,-1,-1/3)$

Table 4. Mass eigenstates in $\tilde{Q}_{\rm L}$ and $\tilde{Q}_{\rm R}$ after the SSB of the trinification symmetry group, and the corresponding tree-level squared masses and U(1) charges. Here, $(\tilde{Q}^I_{\rm LR\pm})^c \equiv \frac{1}{\sqrt{2}}\left[(\tilde{Q}_{\rm L}{}^I)^c_3 \pm \epsilon^{IJ}(\tilde{Q}^*_{\rm R\,J})^c_3\right]$.

3.2 Coloured scalar sector

When $\tilde{L}$ acquires a VEV according to eq. (3.1), all coloured scalar (CS) d.o.f.'s become massive. The mass eigenstates and masses are listed in table 4. Requiring that the squared masses must be non-negative constrains the parameters in V_2 and V_3 as

$$\begin{aligned} \alpha_1 &\geq 2(\lambda_1+\lambda_2+\lambda_3+\lambda_4)\,, \\ \alpha_1+\alpha_2 &\geq 2(\lambda_1+\lambda_2+\lambda_3+\lambda_4)\,, \\ \alpha_1+\alpha_3-\frac{|\gamma|}{\sqrt{2}v_3} &\geq 2(\lambda_1+\lambda_2+\lambda_3+\lambda_4)\,, \\ \alpha_1+\alpha_2+\alpha_3+\alpha_4 &\geq 2(\lambda_1+\lambda_2+\lambda_3+\lambda_4)\,. \end{aligned} \tag{3.7}$$

JHEP09(2016)129

Fields	$(\text{Mass})^2$	$(L+R, X)$	Comment
${G_{\text{C}}}_{\mu}^{1\ldots8}$	0	$(0,0)$	Gauge field of $\text{SU}(3)_{\text{C}}$
${G_{\text{L}}}_{\mu}^{1\ldots3}$	0	$(0,0)$	Gauge field of $\text{SU}(2)_{\text{L}}$
${G_{\text{R}}}_{\mu}^{1\ldots3}$	0	$(0,0)$	Gauge field of $\text{SU}(2)_{\text{R}}$
$\frac{1}{\sqrt{2}}\left({G_{\text{L}}}^{8}+{G_{\text{R}}}^{8}\right)_{\mu}$	0	$(0,0)$	Gauge field of $\text{U}(1)_{\text{L+R}}$
${V_{\text{L}}}_{\mu}^{L}$	$\frac{1}{4}g^2\,v_3^2$	$(+1,+1)$	
${V_{\text{R}}}_{\mu}^{R}$	$\frac{1}{4}g^2\,v_3^2$	$(+1,-1)$	
$V_{\text{s}\mu}$	$\frac{2}{3}g^2\,v_3^2$	$(0,0)$	

Table 5. Gauge boson states after the SSB of the trinification group. All gauge boson states are uncharged under $\{\text{U}(1)_{\text{Z}}\times\text{U}(1)_{\text{B}}\}$.

Fields	$(\text{Mass})^2$	$(L+R, X, Z, B)$	Comment
$({\mathcal{D}_{\text{H}}}^{I})^{c}$	$\frac{1}{2}y^2v_3^2$	$(+2/3,0,0,+1/3)$	Dirac fermion

Table 6. The first and second generation $\text{SU}(2)_{\text{L}}\times\text{SU}(2)_{\text{R}}$-singlet quarks make up an $\text{SU}(2)_{\text{F}}$-doublet Dirac fermion that gets a tree-level mass at the trinification breaking scale. All other fermionic d.o.f.'s in $(L^i)^l_r$, $({Q_{\text{L}}}^i)^c_l$ and $({Q_{\text{R}}}^i)^r_c$ are massless at tree-level.

3.3 Gauge boson sector

After the SSB, nine gauge bosons become massive. Their masses are determined by the trinification gauge coupling g as indicated in table 5. They can be conveniently grouped into two doublets (one for each $\text{SU}(2)_{\text{L,R}}$)

$${V_{\text{L}}}_{\mu}^{L}\equiv\frac{1}{\sqrt{2}}\begin{pmatrix}{G_{\text{L}}}^{6}+\text{i}{G_{\text{L}}}^{7}\\ {G_{\text{L}}}^{4}+\text{i}{G_{\text{L}}}^{5}\end{pmatrix}_{\mu},\quad {V_{\text{R}}}_{\mu}^{R}\equiv\frac{1}{\sqrt{2}}\begin{pmatrix}{G_{\text{R}}}^{6}+\text{i}{G_{\text{R}}}^{7}\\ {G_{\text{R}}}^{4}+\text{i}{G_{\text{R}}}^{5}\end{pmatrix}_{\mu},\tag{3.8}$$

and one singlet

$$V_{\text{s}\mu}\equiv\frac{1}{\sqrt{2}}\left({G_{\text{L}}}^{8}-{G_{\text{R}}}^{8}\right)_{\mu}.\tag{3.9}$$

3.4 Fermion sector

The fermions $(L^i)^l_r$, $({Q_{\text{L}}}^i)^c_l$ and $({Q_{\text{R}}}^i)^r_c$ couple to the scalars $(\tilde{L}^i)^l_r$, $(\tilde{Q}_{\text{L}}{}^i)^c_l$ and $(\tilde{Q}_{\text{R}}{}^i)^r_c$ via the Yukawa interactions given in eq. (2.6). In particular, the VEV leads to a Dirac mass term for one fermionic $\text{SU}(2)_{\text{F}}$ doublet. The corresponding down-type Dirac state is built out of $({Q_{\text{L}}}^I)^c_3$ and $(Q^{\dagger}_{\text{R}\,I})^c_3$ as follows

$$({\mathcal{D}_{\text{H}}}^{I})^{c}\equiv\begin{pmatrix}({Q_{\text{L}}}^{I})^{c}_{3}\\ \epsilon^{IJ}(Q^{\dagger}_{\text{R}\,J})^{c}_{3}\end{pmatrix}.\tag{3.10}$$

The U(1) charges of $\mathcal{D}_{\text{H}}$ are shown in table 6.

3.5 Finding the global minimum through homotopy continuation

If we restrict ourselves to the case of two generations of colour singlet scalars $\tilde{L}^i$ getting VEVs, the most general VEV setting after accounting for gauge [43] and family symmetries can be written as[2]

$$\langle(\tilde{L}^1)^l_r\rangle = \frac{1}{\sqrt{2}}\begin{pmatrix} v^1 & 0 & 0 \\ 0 & v^2 & 0 \\ 0 & 0 & v^3 \end{pmatrix}, \qquad \langle(\tilde{L}^2)^l_r\rangle = \frac{1}{\sqrt{2}}\begin{pmatrix} v^5 & 0 & v^6 \\ 0 & 0 & 0 \\ v^7 & 0 & v^8 \end{pmatrix}. \tag{3.11}$$

Note that, due to $\mathbb{Z}_3$, this choice is physically equivalent to assuming only VEVs in two generations of either $\tilde{Q}_{\rm L}$ or $\tilde{Q}_{\rm R}$.

As discussed in the previous sections, we are interested in the case where only one real scalar field aqcuires a non-zero VEV. The question remains as to whether this is indeed the global minimum of the scalar potential or if the global minimum has a different set of non-zero VEVs and therefore a different symmetry breaking chain takes place.

Using the homotopy continuation method through HOM4PS2 [49], we performed a random scan over 5000 parameter points satisfying the conditions in eqs. (3.6) and (3.7). The homotopy continuation method finds all the solutions of systems of polynomial equations, in this case the minimisation conditions of the tree-level potential (2.3) for the VEV setting in eq. (7.9).

For all the points in the scan, the global minimum was always the one for which $v^3 \equiv v \neq 0$ and $v^{i\neq 3} = 0$, even for parameter points where other minima were present. In other words, for the model described here if we require that there exists a minimum with one real field acquiring a VEV then, excluding pathological cases that might have been missed in the numerical analysis, that minimum is the global one.

The most general case where a third generation is also allowed to acquire VEVs could not be treated with HOM4PS2 due to a complicated system of equations outpacing our computational resources. However, a purely numerical minimisation was performed over a second scan of parameter space leading to the same result as for the case of two generations. Given a parameter point that satisfies the positive scalar mass-squares condition in the one VEV minima, the numerical minimisation procedure was started in a random point in field space, whereby the minimum of the potential was found by a simple steepest-descent method. For the minima obtained in this way, we computed the gauge boson mass spectrum and observed that it numerically matched the masses in table 5. By pretending that $\mathrm{SU}(3)_{\rm F}$ is gauged, we computed the number of unbroken global symmetry generators by counting the number of "new" massless gauge bosons, and could in all cases conclude that it matched the number of global symmetry generators in the effective LR-symmetric model. Therefore, we believe that the all of these minima are related to the one VEV minima in eq. (3.1) by a symmetry transformation, and are hence physically equivalent.

[2]Using the $\mathrm{SU}(2)_{\rm F} \subset \mathrm{SU}(3)_{\rm F}$ family symmetry we can "rotate away" one of the VEVs of the general case shown in ref. [43].

JHEP09(2016)129

4 The low-scale effective LR-symmetric model

4.1 Minimal particle content of the effective model

The trinification group is spontaneously broken by the VEV v_3 in eq. (3.1) to the following symmetry

$$\mathrm{SU(3)_C \times SU(2)_L \times SU(2)_R \times U(1)_{L+R} \times \{SU(2)_F \times U(1)_X \times U(1)_Z \times U(1)_B\}}. \tag{4.1}$$

The decomposition of $\tilde{L}$ in terms of representations of the group (4.1) can be written as

$$\begin{aligned}(\tilde{L}^i)^l_r = \delta^i_I \Big[\delta^l_L \delta^R_r\, (\tilde{H}^I)^L_R + \delta^l_L \delta^3_r\, (\tilde{l}_{\mathrm{L}}{}^I)^L + \delta^l_3\, \delta^R_r (\tilde{l}_{\mathrm{R}}{}^I)_R + \delta^l_3 \delta^3_r\, \tilde{\Phi}^I\Big] \\ + \delta^i_3 \left[\delta^l_L \delta^R_r\, \tilde{h}^L_R + \delta^l_L \delta^3_r\, \tilde{l}^{s\,L}_{\mathrm{L}} + \delta^L_3 \delta^R_r\, \tilde{l}^s_{\mathrm{R}R} + \delta^l_3 \delta^3_r \left(\tilde{\Phi}^s + \frac{v_3}{\sqrt{2}}\right)\right].\end{aligned} \tag{4.2}$$

Here, $\tilde{l}^s_{\mathrm{L,R}}$ and $\mathrm{Im}[\tilde{\Phi}^s]$ are the gauge Goldstone d.o.f.'s that become the longitudinal polarisation states of the heavy vector bosons listed in table 5, wheras $\tilde{\Phi}^I$ is the "global" Goldstone boson. Similarly, the fermion multiplet L can be written in terms of reps of the new symmetry group as follows

$$\begin{aligned}(L^i)^l_r = \delta^i_I \Big[\delta^l_L \delta^R_r\, (H^I)^L_R + \delta^l_L \delta^3_r\, (l_{\mathrm{L}}{}^I)^L + \delta^l_3 \delta^R_r\, (l_{\mathrm{R}}{}^I)_R + \delta^l_3 \delta^3_r\, \Phi^I\Big] \\ + \delta^i_3 \Big[\delta^l_L \delta^R_r\, (H^s)^L_R + \delta^l_L \delta^3_r\, l^{s\,L}_{\mathrm{L}} + \delta^l_3 \delta^R_r\, l^s_{\mathrm{R}R} + \delta^l_3 \delta^3_r\, \Phi^s\Big].\end{aligned} \tag{4.3}$$

Moreover, the decomposition of the trinification quark multiplets, Q_{L} and Q_{R}, reads

$$\begin{aligned}(Q_{\mathrm{L}}{}^i)^c_l &= \delta^i_I \left[\delta^L_l\, (\mathcal{Q}_{\mathrm{L}}{}^I)^c_L + \delta^3_l\, (D_{\mathrm{L}}{}^I)^c\right] + \delta^i_3 \left[\delta^L_l\, \mathcal{Q}^{s\,c}_{\mathrm{L}L} + \delta^3_l\, D^{s\,c}_{\mathrm{L}}\right], \\ (Q_{\mathrm{R}}{}^i)^r_c &= \delta^i_I \left[\delta^r_R\, (\mathcal{Q}_{\mathrm{R}}{}^I)^R_c + \delta^r_3 (D_{\mathrm{R}}{}^I)_c\right] + \delta^i_3 \left[\delta^r_R\, \mathcal{Q}^{s\,R}_{\mathrm{R}c} + \delta^r_3\, D^s_{\mathrm{R}c}\right],\end{aligned} \tag{4.4}$$

and similarly for $\tilde{Q}_{\mathrm{L,R}}$.

As mentioned in section 3, we want to explore whether a radiatively induced breaking down to the SM gauge group can happen for the proposed model. As will be discussed later in detail, in order for that to happen, we need to have at least one $\mathrm{SU(2)_R}$ and one $\mathrm{SU(2)_L}$ scalar doublet in the effective theory so that the $\mathrm{SU(2)_R}$-doublet mass parameter can run negative. With this in mind, and considering the simplest possible scenario, we will focus our attention on a subset of the parameter space where after the trinification symmetry is broken, the scalar spectrum comprises two very light states, namely,

$$\tilde{h}^L_R \equiv (\tilde{L}^3)^L_R \qquad \text{and} \qquad (\tilde{l}_{\mathrm{R}}{}^I)_R \equiv (\tilde{L}^I)^3_R\,, \tag{4.5}$$

in addition to the global Goldstone field $\tilde{\Phi}^I \equiv (\tilde{L}^I)^3_3$. The remaining scalars either get masses of $\mathcal{O}(v_3)$ or get "eaten" by heavy gauge bosons. For this particular case, one can integrate out all the heavy scalars ending up with a simpler effective theory containing the light and massless fields only. In the fermion sector, the fields $(Q_{\mathrm{L}}{}^I)^c_3$ and $(Q_{\mathrm{R}}{}^I)^3_c$ can also be integrated out as they make up the heavy Dirac fermions shown in table 6. The fields that are present in the effective theory are shown in table 7.

JHEP09(2016)129

In order to parametrize the relevant regions of parameter space giving rise to such a minimal particle content of the effective model, let us define small dimensionless δ and ε parameters as follows

$$\varepsilon \equiv -\lambda_2 - \lambda_3\,, \quad \delta \equiv -\lambda_3 - \lambda_4, \tag{4.6}$$

such that $m_R^2 = \varepsilon v_3^2$ and $m_h^2 = \delta v_3^2$. We will then construct the effective LR-symmetric model assuming $\varepsilon \ll 1$ and $\delta \ll 1$. At higher orders in perturbation theory, other tree-level couplings (such as α_i and γ) will enter in the full expressions for $m_{h,R}^2$. To still keep these states sufficiently light at the matching scale will then further constrain the parameter space as the simple assumptions $\varepsilon, \delta \ll 1$ will not suffice. This is further discussed in section 7.2.

In the LR-symmetric effective model, the fields interact with gauge bosons according to their representations under the gauge groups as given in table 7, with strengths determined by the gauge couplings $g_{\rm L}$, $g_{\rm R}$, $g_{\rm C}$ and $g_{\rm L+R}$. At the matching scale v_3, these are related to the trinification gauge coupling g as

$$g_{\rm L} = g_{\rm R} = g_{\rm C} = g\,, \quad g_{\rm L+R} = \sqrt{\frac{3}{8}}\,g\,. \tag{4.7}$$

4.2 Matching of the scalar potential parameters

The GUT-scale scalar potential V should be matched onto the most general renormalizable scalar potential for $\tilde{h}_R^L$, $(\tilde{l}_{\rm R}{}^I)_R$ and $\tilde{\Phi}^I$ in the low-energy LR-symmetric model:

$$\begin{aligned}
V_{LR} = {} & m_h^2\,|\tilde{h}|^2 + m_R^2\,|\tilde{l}_{\rm R}|^2 + m_{\tilde{\Phi}}^2\,|\tilde{\Phi}|^2 \\
& + \lambda_a\,|\tilde{h}|^4 + \lambda_b\,|\tilde{l}_{\rm R}|^4 + \lambda_c\,|\tilde{\Phi}|^4 + \lambda_d\,|\tilde{h}|^2|\tilde{\Phi}|^2 + \lambda_e\,|\tilde{l}_{\rm R}|^2|\tilde{\Phi}|^2 + \lambda_f\,|\tilde{l}_{\rm R}|^2|\tilde{h}|^2 \\
& + \lambda_g\,(\tilde{l}_{\rm R}{}^I)_{R_1}\;(\tilde{l}^*_{\rm R}{}_I)^{R_2}\;\tilde{h}^{L}_{R'_1}\;\tilde{h}^{*R'_2}_{\quad L}\quad \epsilon^{R_1R'_1}\,\epsilon_{R_2R'_2} \\
& + \lambda_h\,(\tilde{l}_{\rm R}{}^{I_1})_R\;(\tilde{l}^*_{\rm R}{}_{J_1})^{R}\;\tilde{\Phi}^{I_2}\;\tilde{\Phi}^*_{J_2}\quad \epsilon_{I_1I_2}\,\epsilon^{J_1J_2} \\
& + \lambda_i\,(\tilde{l}_{\rm R}{}^{I_1})_{R_1}\;(\tilde{l}_{\rm R}{}^{I_2})_{R'_1}\;(\tilde{l}^*_{\rm R}{}_{J_1})^{R_2}\;(\tilde{l}^*_{\rm R}{}_{J_2})^{R'_2}\quad \epsilon_{I_1I_2}\,\epsilon^{J_1J_2}\,\epsilon_{R_2R'_2}\,\epsilon^{R_1R'_1} \\
& + \lambda_j\,\tilde{h}^{L_1}_{R_1}\;\tilde{h}^{L'_1}_{R'_1}\;\tilde{h}^{*R_2}_{\quad L_2}\;\tilde{h}^{*R'_2}_{\quad L'_2}\quad \epsilon_{L_1L'_1}\,\epsilon^{L_2L'_2}\,\epsilon_{R_2R'_2}\,\epsilon^{R_1R'_1}
\end{aligned} \tag{4.8}$$

The tree-level matching conditions in the scalar sector are obtained by requiring that the n-point functions with external scalars in the high-scale and the low-scale theory coincide at tree-level at the matching scale μ_m, which we take to be the trinification breaking scale v_3. In this case, we get all relations between the high scale parameters $\{v_3, \lambda_{1,3}, \epsilon, \delta\}$, and the low-scale parameters $\{m^2_{h,R,\tilde{\Phi}}, \lambda_{a,\ldots,j}\}$ from the two-point functions (i.e. from the masses squared) and the four-point functions (quartic couplings). We compute the four-point functions taking the limit of small external momenta (compared to v_3 scale), since we are only interested in the matching of the renormalizable operators. Any momentum dependence in the four-point functions in the low-scale theory would instead be attributed to (non-renormalizable) derivative interactions. We do not take these higher order derivative operators into account since they presumably would have a negligible effect in the infrared

JHEP09(2016)129

behaviour of the theory. Thus, the matching conditions are

$$\begin{aligned}
&m_h^2 = \delta v^2\,, \quad m_R^2 = \varepsilon v^2\,, \quad m_{\tilde{\Phi}}^2 = 0\,,\\
&\lambda_c = \lambda_d = \lambda_e = \lambda_h = 0\,,\\
&\lambda_g = -2\lambda_3\,, \quad \lambda_i = \frac{1}{2}\varepsilon\,, \quad \lambda_j = \frac{1}{2}\delta\,,\\
&\lambda_a = \lambda_1 - \lambda_3 - \varepsilon - \delta - \frac{(\lambda_1 - \lambda_3 - \varepsilon)^2}{\lambda_1 - \lambda_3 - \varepsilon - \delta} \approx -2\delta + \mathcal{O}(\varepsilon^2, \varepsilon\delta, \delta^2)\,,\\
&\lambda_b = \lambda_1 - \lambda_3 - \varepsilon - \delta - \frac{(\lambda_1 - \lambda_3 - \delta)^2}{\lambda_1 - \lambda_3 - \varepsilon - \delta} \approx -2\varepsilon + \mathcal{O}(\varepsilon^2, \varepsilon\delta, \delta^2)\,,\\
&\lambda_f = 2\left[\lambda_1 + \lambda_3 - \frac{(\lambda_1 - \lambda_3 - \varepsilon)(\lambda_1 - \lambda_3 - \delta)}{\lambda_1 - \lambda_3 - \varepsilon - \delta}\right] \approx 4\lambda_3 + \mathcal{O}(\varepsilon^2, \varepsilon\delta, \delta^2)\,.
\end{aligned} \tag{4.9}$$

Interestingly, all λ_1's cancel out in the matching conditions, provided that ε and δ are sufficiently small, which means that λ_1 does not affect the values of the couplings in the effective LR-symmetric model at tree-level. This can be seen as a consequence of $\tilde{h}_R^L$, $(\tilde{l}_{\mathrm{R}}{}^I)_R$ and $\tilde{\Phi}^I$ becoming Goldstone bosons of the O(54) $\to$ O(53) breaking that is induced in the CSS sector by the v_3 VEV in the limit λ_2, λ_3, $\lambda_4 \to 0$ (since they are Goldstone bosons in this limit, they must decouple from the scalar potential in the same limit).

4.3 Fermion sector

Though the trinification theory only contains one Yukawa coupling, many terms are allowed by the symmetry group of the LR-symmetric effective model in the fermion sector:

$$\begin{aligned}
\mathcal{L}_{\mathrm{Fermion}}^{(LR)} = {} & Y_\alpha\, (\tilde{l}^*_{\mathrm{R}I})^R\, (l_{\mathrm{R}}{}^I)_R\, \Phi^s + Y_\beta\, (\tilde{l}^*_{\mathrm{R}I})^R\, l^s_{\mathrm{R}R}\, \Phi^I + Y_\gamma\, (\tilde{l}_{\mathrm{R}}{}^I)_R\, (\mathcal{Q}_{\mathrm{R}}{}^J)^R\, D^s_{\mathrm{L}}\, \epsilon_{IJ}\\
& + Y_\delta\, \tilde{h}^{*R}_L\, (H^s)^L_R\, \Phi^s + Y_\epsilon\, \tilde{h}^{*R}_L\, l^{s\,L}_{\mathrm{L}}\, l^s_{\mathrm{R}R} + Y_\zeta\, \tilde{h}^L_R\, (\mathcal{Q}_{\mathrm{L}}{}^I)_L\, (\mathcal{Q}_{\mathrm{R}}{}^J)^R\, \epsilon_{IJ}\\
& + Y_\eta\, \tilde{\Phi}^*_I\, \Phi^I \Phi^s + \frac{m_{\Phi^s}}{2}\, \Phi^s \Phi^s + \mathrm{c.c.}
\end{aligned} \tag{4.10}$$

The matching conditions for these Yukawa couplings are rather easy at tree-level, as only two of them are found to have non-vanishing values at the matching scale. This does not mean that the other couplings are not present in the effective theory and it would be a subject of a future study to calculate the matching conditions at higher orders where they might not necessarily vanish. However, for the purpose of this work, which is to explore a potential for the radiative breaking of the LR symmetry down to the SM gauge group, the tree-level approximation is expected to be sufficient. In this case, the matching conditions are such that

$$Y_\zeta = -y \qquad \text{and} \qquad Y_\gamma = y\,, \tag{4.11}$$

while $Y_{\alpha,\beta,\delta,\epsilon,\eta} = 0$. Furthermore, the β-functions in appendix A indicate that the Yukawa couplings that are zero at the matching scale will also remain zero at lower scales, since $\beta_{Y_i} \propto Y_i$.

With the matching conditions defined above, the parameters of the effective LR-symmetric model can be determined from a reduced set of parameters of the GUT-scale theory. The vacuum stability constraints (3.6) and (3.7) can be then translated as well to

JHEP09(2016)129

reduce further the allowed parameter space for the effective theory. With this framework in mind, the question remains as to whether the remaining symmetries of the effective theory can be broken radiatively by one-loop RG running at a lower scale leading to an effective model which approaches the SM.

4.4 Decoupling of "global" Goldstone bosons

It can be shown, on very general grounds that Goldstone bosons appearing due to the spontaneous breaking of a global symmetry at a scale v_3, have negligibly small interactions at scales $\mu \ll v_3$ [50, 51]. This decoupling is obvious if one chooses a specific exponential representation of the Goldstone d.o.f.'s, which comes at expense of manifest renormalisability. In this work, we have instead chosen the simple (but equivalent) linear representation of the global Goldstone d.o.f.'s $\tilde{\Phi}^I$ such that renormalisability (but not decoupling) is manifest in the GUT-scale trinification theory. Nevertheless, with the results from the three previous sections, we can see explicitly how $\tilde{\Phi}^I$ decouple at scales well below v_3.

Firstly, we notice that $\tilde{\Phi}^I$ decouples from the scalar potential at the matching scale since $m_{\tilde{\Phi}} = 0$ and $\lambda_c = \lambda_d = \lambda_e = \lambda_h = 0$. Instead, one finds that for the matching to agree at non-zero Goldstone boson momenta, one has to introduce derivative interactions among the Goldstone bosons as well as between the Goldstone bosons and non-Goldstone fields. These derivative interactions necessarily have dim > 4 and hence must be suppressed by the trinification breaking scale $\sim v_3$. Since these operators presumably will be increasingly irrelevant in the infrared, we simply omit them from our LR-symmetric effective Lagrangian.

In the trinification fermion sector shown in eq. (2.6), one can check that the only Yukawa interactions involving $\tilde{\Phi}^I$ that are non-zero at tree-level also involve the heavy quark fields $(Q_{\mathrm{L}}{}^I)^c_3$ and $(Q_{\mathrm{R}}{}^I)^3_c$ (which are integrated out at the trinification breaking scale). In addition, in the effective theory, one new Yukawa interaction with $\tilde{\Phi}^I$ is allowed by symmetry (Y_η in eq. (4.10)), but it vanishes at the matching scale. The corresponding β-function, β_{Y_η}, is proportional to Y_η, meaning that the vanishing matching condition also forces $Y_\eta = 0$ at lower scales.

Having shown the disappearance of scalar and Yukawa interactions with $\tilde{\Phi}^I$, only gauge interactions remain. However, since $\tilde{\Phi}^I$ is a gauge singlet, it will neither interact via gauge interactions nor contribute to the running of the gauge couplings in the effective LR-symmetric model.

5 Breaking of $\mathrm{SU(2)_R \times U(1)_{L+R}}$ in the effective model

In order to reproduce the phenomenology of the SM at low energies, the gauge $\mathrm{SU(2)_R \times U(1)_{L+R}}$ subgroup needs to be broken to the SM hypercharge group $\mathrm{U(1)_Y}$. One of the persistent issues in high energy models is the fact that the vastly different energy scales associated have to be given through input parameters. One way of dealing with this issue is to introduce the possibility of radiative symmetry breaking, i.e SSB triggered by the RG evolution of the model. This is a standard way of understanding, for example, EW symmetry breaking in the MSSM where the running of $m^2_{H_u}$ drives the breaking of $\mathrm{SU(2)_L \times U(1)_Y}$ [52–54]. The question remains as to whether this model offers a possibility

JHEP09(2016)129

	$SU(2)_L$	$SU(2)_R$	$SU(3)_C$	$U(1)_{L+R}$	$\{SU(2)_F\}$	$\{U(1)_X\}$	$\{U(1)_Z\}$	$\{U(1)_B\}$
fermions								
H	**2**	$\bar{\mathbf{2}}$	**1**	0	**2**	0	+1	0
l_L	**2**	**1**	**1**	+1	**2**	−1	+1	0
l_R	**1**	$\bar{\mathbf{2}}$	**1**	−1	**2**	−1	+1	0
Φ	**1**	**1**	**1**	0	**2**	−2	+1	0
$\mathcal{Q}_L$	$\bar{\mathbf{2}}$	**1**	**3**	−1/3	**2**	−1	0	+1/3
$\mathcal{Q}_R$	**1**	**2**	$\bar{\mathbf{3}}$	+1/3	**2**	−1	0	−1/3
H^s	**2**	$\bar{\mathbf{2}}$	**1**	0	**1**	+2	0	0
l_L^s	**2**	**1**	**1**	+1	**1**	+1	0	0
l_R^s	**1**	$\bar{\mathbf{2}}$	**1**	−1	**1**	+1	0	0
Φ^s	**1**	**1**	**1**	0	**1**	0	0	0
$\mathcal{Q}_L^s$	$\bar{\mathbf{2}}$	**1**	**3**	−1/3	**1**	+1	−1	+1/3
$\mathcal{Q}_R^s$	**1**	**2**	$\bar{\mathbf{3}}$	+1/3	**1**	+1	−1	−1/3
D_L^s	**1**	**1**	**3**	+2/3	**1**	+2	−1	+1/3
D_R^s	**1**	**1**	$\bar{\mathbf{3}}$	−2/3	**1**	+2	−1	−1/3
scalars								
$\tilde{h}$	**2**	$\bar{\mathbf{2}}$	**1**	0	**1**	+2	0	0
$\tilde{l}_R$	**1**	$\bar{\mathbf{2}}$	**1**	−1	**2**	−1	+1	0
$\tilde{\Phi}$	**1**	**1**	**1**	0	**2**	−2	+1	0
gauge bosons								
G_L	**3**	**1**	**1**	0	**1**	0	0	0
G_R	**1**	**3**	**1**	0	**1**	0	0	0
G_C	**1**	**1**	**8**	0	**1**	0	0	0
G_{L+R}	**1**	**1**	**1**	0	**1**	0	0	0

Table 7. Field content of the effective LR-symmetric model.

of breaking $SU(2)_R \times U(1)_{L+R}$ through the RG running of m_R^2 and the rest of parameters of the effective model with initial conditions coming from tree-level matching of the high energy theory. This will give us the possibility of checking under which conditions (for the high-energy input parameters) this radiative breaking can be induced.

For this purpose, we consider two separate scenarios. In scenario I, we study the properties of a minimum in the scalar potential of the effective LR-symmetric model where $SU(2)_R \times U(1)_{L+R}$ is broken to the analogous of $U(1)_Y$ in the SM, (i.e. the EW gauge group $SU(2)_L \times U(1)_Y$ is unbroken in this minimum). To study the model at the electro-weak scale, where $SU(2)_L \times U(1)_Y$ is broken, a second step of matching and running would have to be performed to discover whether there is a sign change of the Higgs squared mass

JHEP09(2016)129

parameter inducing the electro-weak symmetry breaking. In scenario II, we instead study minima with a more complicated VEV structure such that $\mathrm{SU}(2)_\mathrm{L} \times \mathrm{SU}(2)_\mathrm{R} \times \mathrm{U}(1)_{\mathrm{L+R}}$ is directly broken down to $\mathrm{U}(1)_{\mathrm{E.M.}}$. This is accomplished by suitable VEVs both in $\tilde{h}$ and in $\tilde{l}_\mathrm{R}$. The VEV in $\tilde{l}_\mathrm{R}$ needs to be larger than the Higgs VEV to keep the W' and Z' bosons heavy, but not too large as to ruin the convergence the perturbative expansion through large logarithms of the ratio between the two VEVs. If this ratio would become too large, Scenario I is more appropriate.

5.1 Scenario I: breaking to the SM gauge group

Let us first understand what are the conditions necessary for $\mathrm{SU}(2)_\mathrm{R} \times \mathrm{U}(1)_{\mathrm{L+R}}$ breaking through non-vanishing VEV for the scalar field $\tilde{l}_\mathrm{R}$,

$$\langle (\tilde{l}_\mathrm{R}{}^I)_R \rangle = \delta_2^I \delta_R^2 \frac{w}{\sqrt{2}} = \begin{pmatrix} 0 & 0 \\ 0 & \frac{w}{\sqrt{2}} \end{pmatrix}, \tag{5.1}$$

where w is taken to be real. The extremal condition for such a VEV setting reads

$$-m_R^2 = \lambda_b w^2. \tag{5.2}$$

This leaves the following gauged U(1) generator unbroken,

$$T_\mathrm{Y} = T_\mathrm{R}^3 + \frac{1}{2} T_{\mathrm{L+R}}, \tag{5.3}$$

which can be identified as the SM hypercharge generator. In addition, eq. (5.1) leaves four global U(1) generators unbroken,

$$T_\mathrm{D} \equiv \frac{1}{2}\left(T_\mathrm{X} - T_{\mathrm{L+R}}\right), \quad T_\mathrm{E} \equiv T_\mathrm{F}^3 + \frac{1}{2} T_\mathrm{Z}, \quad T_\mathrm{G} \equiv \frac{1}{2}\left(T_\mathrm{Z} + T_{\mathrm{L+R}}\right), \quad T_\mathrm{B}. \tag{5.4}$$

Thus, the VEV (5.1) breaks the LR symmetry group (4.1) down to

$$\mathrm{SU}(3)_\mathrm{C} \times \mathrm{SU}(2)_\mathrm{L} \times \mathrm{U}(1)_\mathrm{Y} \times \{\mathrm{U}(1)_\mathrm{D} \times \mathrm{U}(1)_\mathrm{E} \times \mathrm{U}(1)_\mathrm{G} \times \mathrm{U}(1)_\mathrm{B}\}. \tag{5.5}$$

which will also be the symmetry group of a SM-like effective model that is obtained when the heavy particles in the effective LR-symmetric model are integrated out.

The scalar mass eigenstates in the minimum described by eq. (5.2) are shown in table 8. Notice, in particular, that the scalar spectrum contains one massless complex d.o.f. that is the "global" Goldstone boson from the breaking of the global part of the LR symmetry. We expect this to decouple at scales $\mu \ll w$, similarly to how $\tilde{\Phi}^I$ decouples for $\mu \ll v$.

The gauge fields after SSB of the LR symmetry are mixed and give rise to the massive and massless states shown in table 9. The massless states are the gauge fields of the unbroken gauge symmetries, and the massive gauge fields are the combinations

$$W'^{\pm}{}_\mu = \frac{1}{\sqrt{2}}\left(G_\mathrm{R}{}^1 \mp \mathrm{i} G_\mathrm{R}{}^2\right)_\mu, \quad Z'^0{}_\mu = \cos\theta_V \, G_{\mathrm{L+R}\mu} - \sin\theta_V \, G_{\mathrm{R}\mu}^3 \tag{5.6}$$

JHEP09(2016)129

Fields	$(\text{Mass})^2$	(Y, D, E)	Comment
$\tilde{h}_1^L$	$m_{h_2}^2 \equiv m_h^2 + \frac{1}{2}(\lambda_g - \lambda_f)w^2$	$(-1/2, +1, 0)$	
$\tilde{h}_2^L$	$m_{h_1}^2 \equiv m_h^2 - \frac{1}{2}\lambda_f w^2$	$(+1/2, +1, 0)$	
$(\tilde{l}_{\rm R}{}^1)_1$	$m_{r_2}^2 \equiv 2\lambda_i w^2$	$(-1, 0, +1)$	
$\text{Re}[(\tilde{l}_{\rm R}{}^2)_2]$	$m_{r_1}^2 \equiv 2\lambda_b w^2$	$(0, 0, 0)$	
$(\tilde{l}_{\rm R}{}^2)_1$	0	$(-1, 0, 0)$	Gauge Goldstone
$\text{Im}[(\tilde{l}_{\rm R}{}^2)_2]$	0	$(0, 0, 0)$	Gauge Goldstone
$(\tilde{l}_{\rm R}{}^1)_2$	0	$(0, 0, +1)$	Global Goldstone

Table 8. Mass eigenstates in $\tilde{h}$ and $\tilde{l}_{\rm R}$ after SSB of the LR symmetry by $\tilde{l}_{\rm R}$ VEV, the corresponding tree-level masses and U(1) charges. All scalars are uncharged under the $\{\text{U}(1)_{\rm G} \times \text{U}(1)_{\rm B}\}$ global symmetry.

Fields	$(\text{Mass})^2$	Y	Comment
${G_{\rm C}}_\mu^{1,\ldots,8}$	0	0	Gauge field of $\text{SU}(3)_{\rm C}$
${G_{\rm L}}_\mu^{1,2,3}$	0	0	Gauge field of $\text{SU}(2)_{\rm L}$
$s_{\theta_V} G_{{\rm L+R}\mu} + c_{\theta_V} {G_{\rm R}}_\mu^3$	0	0	Gauge field of $\text{U}(1)_{\rm Y}$
${W'^{\pm}}_\mu$	$m_{W'}^2 \equiv \frac{1}{4} g_{\rm R}^2 w^2$	± 1	
${Z'^0}_\mu$	$m_{Z'}^2 \equiv \left(g_{\rm L+R}^2 + \frac{1}{4} g_{\rm R}^2\right) w^2$	0	

Table 9. Gauge boson mass eigenstates and their hypercharges after the spontaneous LR symmetry breaking. All gauge bosons are uncharged under the global $\{\text{U}(1)_{\rm D} \times \text{U}(1)_{\rm E} \times \text{U}(1)_{\rm G} \times \text{U}(1)_{\rm B}\}$ group. Here, $c_{\theta_V} \equiv \cos\theta_V$ and $s_{\theta_V} \equiv \sin\theta_V$.

with $\tan\theta_V = g_{\rm R}/2g_{\rm L+R}$. The hypercharge gauge coupling $g_{\rm Y}$ becomes

$$g_{\rm Y} = \frac{2\, g_{\rm R}\, g_{\rm L+R}}{\sqrt{4g_{\rm L+R}^2 + g_{\rm R}^2}}. \tag{5.7}$$

For general values of the Yukawa couplings in eq. (4.10), many fermion fields become massive once $\langle \tilde{l}_{\rm R} \rangle \neq 0$. However, in the approximation employed in this work, i.e. tree-level matching and one-loop RG evolution, most of the Yukawa couplings are zero and only one Dirac fermion becomes massive in the effective LR-symmetric model (shown in table 10). This fermion is a Dirac state

$$\mathcal{D}_{\rm s}{}^c \equiv \begin{pmatrix} D_{\rm L}^{s\,c} \\ (\mathcal{Q}_{\rm R}^{\dagger\,1})_c^2 \end{pmatrix} \tag{5.8}$$

and, when integrated out, leaves behind three $\text{SU}(2)_{\rm L}$ doublet quarks and six $\text{SU}(2)_{\rm L}$ singlet quarks that will make up the SM quark sector.

5.2 Scenario II: breaking directly to $\text{U}(1)_{\rm E.M.}$

A second possible scenario is that in which both $(\tilde{l}_{\rm R}{}^I)_R$ and $\tilde{h}_R^L$ develop VEVs, which would directly trigger $\text{SU}(2)_{\rm L} \times \text{SU}(2)_{\rm R} \times \text{U}(1)_{\rm L+R} \to \text{U}(1)_{\rm E.M.}$. Although this case is

JHEP09(2016)129

Fields	$(\text{Mass})^2$	(Y, D, E)
${\mathcal{D}_{\text{s}}}^c$	$m_q^2 \equiv \frac{1}{2} Y_\gamma^2 w^2$	$(+1/3, 2/3, -1/3)$

Table 10. Massive quark field and its quantum numbers after the $\text{SU}(2)_{\text{R}} \times \text{U}(1)_{\text{L+R}}$ breaking.

certainly allowed by the model, and might also be triggered by RG running of effective Lagrangian parameters, there is no a priori reason that there will be any hierarchy in the VEVs of the fields consistent with the SM. This could lead to several massive gauge bosons with comparable masses which would immediately be in conflict with what is observed experimentally. So far, only the SM $W^\pm$ and Z^0 bosons have been observed, and the existing LHC bounds on extra gauge bosons [55, 56] would force an unnatural hierarchy which is precisely the problem one wants to avoid by means of radiative breaking.

Nevertheless, let us explore the conditions under which such symmetry breaking might lead to an unbroken $\text{U}(1)_{\text{E.M.}}$. The most general VEV setting, after accounting for gauge symmetries for $({\tilde{l}_{\text{R}}}^I)_R$ and $\tilde{h}_R^L$ would be:

$$\langle ({\tilde{l}_{\text{R}}}^I)_R \rangle = \frac{1}{\sqrt{2}} \begin{pmatrix} w_1 & w_2 \\ 0 & w_3 \end{pmatrix} \qquad \langle \tilde{h}_R^L \rangle = \frac{1}{\sqrt{2}} \begin{pmatrix} v_1 & 0 \\ 0 & v_2 \end{pmatrix}. \tag{5.9}$$

However, not all of these minima lead to a $\text{U}(1)_{\text{E.M.}}$ remaining gauge symmetry consistent with the proposed framework. To understand this, it is useful to think as if the VEVs are attained sequentially. Let us assume $({\tilde{l}_{\text{R}}}^I)_R$ gets its VEV first. From our previous analysis we know that in order to identify $T_{\text{E.M.}} = T_{\text{L}}^3 + T_{\text{Y}}$ we need $\tilde{h}_R^L$ to break down to two $\text{SU}(2)_{\text{L}}$ doublets with opposite hypercharge. This is only possible with $w_1 = w_2 = 0$ (up to any symmetry transformation on $\langle \tilde{l}_{\text{R}} \rangle$). Once $({\tilde{l}_{\text{R}}}^I)_R$ has obtained its VEV, there are physically different VEV settings in the Higgs bi-doublet we should explore separately: $v_1 = v \neq 0$ and $v_2 = 0$ (Case A), $v_2 = v \neq 0$ and $v_1 = 0$ (Case B), and $v_1 \neq 0$ and $v_2 \neq 0$ (Case C). In the following we will explore the details of Case A and B. Case C, where both Higgs VEVs are non-zero, is cumbersome and can be left for a future work. The reason for this is that for that case the masses in the scalar sector can not be obtained analytically and the type of analysis we will do in section 6.1.1 is not feasible without further work. We will thus take a closer look at scenario I and the first two cases described above.

5.2.1 Case A

Given the VEV setting

$$\langle ({\tilde{l}_{\text{R}}}^I)_R \rangle = \begin{pmatrix} 0 & 0 \\ 0 & \frac{w}{\sqrt{2}} \end{pmatrix}, \qquad \langle \tilde{h}_R^L \rangle = \begin{pmatrix} 0 & 0 \\ 0 & \frac{v}{\sqrt{2}} \end{pmatrix}, \tag{5.10}$$

the extremal conditions become

$$\left(m_h^2 + v^2 \lambda_a - \frac{1}{2} w^2 \lambda_f \right) v = 0\,, \quad \left(m_R^2 + w^2 \lambda_b - \frac{1}{2} v^2 \lambda_f \right) w = 0. \tag{5.11}$$

JHEP09(2016)129

With $v \neq 0$ and $w \neq 0$, there is only one unbroken gauge symmetry generator

$$T_{\text{E.M.}} = T_{\text{L}}^3 + T_{\text{R}}^3 + \frac{1}{2} T_{\text{L+R}} \tag{5.12}$$

which corresponds exactly to the generator of $\text{U}(1)_{\text{E.M}}$ in our previous analysis with only $(\tilde{l}_{\text{R}}{}^I)_R$ VEV. There are also two new U(1) global symmetries in addition to $\{\text{U}(1)_{\text{G}} \times \text{U}(1)_{\text{B}}\}$ with generators

$$T_{\text{V}} = T_{\text{X}} - T_{\text{L+R}} + 4T_{\text{L}}^3\,, \quad T_{\text{W}} = T_{\text{F}}^3 - \frac{1}{2} T_{\text{L+R}} \tag{5.13}$$

The mass eigenstates in the scalar sector after this symmetry breaking are shown in table 11. In particular, there is one real state which obtains a mass of $\mathcal{O}(v)$ when $v \ll w$, which would be the candidate for the 125 GeV SM Higgs particle.

5.2.2 Case B

A second possible case follows from the VEV assignment

$$\langle (\tilde{l}_{\text{R}}{}^I)_R \rangle = \begin{pmatrix} 0 & 0 \\ 0 & \frac{w}{\sqrt{2}} \end{pmatrix} \qquad \langle \tilde{h}_R^L \rangle = \begin{pmatrix} \frac{v}{\sqrt{2}} & 0 \\ 0 & 0 \end{pmatrix}. \tag{5.14}$$

The extremal conditions in this case will be

$$\left(m_H^2 + v^2 \lambda_a + \frac{1}{2} w^2 (-\lambda_f + \lambda_g) \right) v = 0\,, \quad \left(m_R^2 + w^2 \lambda_b + \frac{1}{2} v^2 (-\lambda_f + \lambda_g) \right) w = 0. \tag{5.15}$$

The mass eigenstates in the scalar sector after this symmetry breaking are shown in table 12, where as in the previous case the spectrum contains a candidate for the SM Higgs particle. The VEV setting (5.14) leaves the same gauged $\text{U}(1)_{\text{E.M.}}$ and global $\text{U}(1)_{\text{W}}$ unbroken as the vev setting in eq. (5.10). However, the $\text{U}(1)_{\text{V}}$ is replaced by $\text{U}(1)_{\text{V}'}$ which is generated by

$$T_{\text{V}'} = T_{\text{X}} - T_{\text{L+R}} - 4T_{\text{L}}^3\,. \tag{5.16}$$

6 Numerical results

The main question to answer for the proposed framework is whether for a consistent set of parameters of the trinification theory, the RG running in the effective LR-symmetric theory can trigger the radiative breaking of $\text{SU}(2)_{\text{R}} \times \text{U}(1)_{\text{L+R}}$, and for what regions in parameter space this happens. In addition, we will explore under which circumstances we can get close to a realistic SM-like scalar sector, with a light $\text{SU}(2)_{\text{L}}$ scalar doublet with hypercharge $Y = +1/2$ remaining in the spectrum at lower energies (which potentially can induce EW symmetry breaking). The resulting low-scale mass spectrum after the radiative symmetry breaking will depend on our choice of initial parameters only, but the connection between the initial values of the parameters and the resulting mass spectrum is not obvious. In order to explore it, we implemented a parameter scanning framework using numerical integration of the RG equations together with a simulated annealing (SA) procedure to scan over the possible initial values of high-scale parameters.

We calculated one-loop β-functions for the effective LR-symmetric model using the package `pyr@te` [57], which are written in appendix A.

JHEP09(2016)129

Fields	$(\text{Mass})^2$	Comment
$s_\alpha(\tilde{l}_{\rm R}{}^2)_1 - c_\alpha \tilde{h}_1^2$	$\frac{1}{2}(v^2+w^2)\lambda_g$	
$(\tilde{l}_{\rm R}{}^1)_1$	$\frac{1}{2}v^2\lambda_g + 2w^2\lambda_i$	
$\tilde{h}_1^1$	$\frac{1}{2}w^2\lambda_g + 2v^2\lambda_j$	
$c_\eta \text{Re}[\tilde{h}_2^2] + s_\eta \text{Re}[(\tilde{l}_{\rm R}{}^2)_2]$	$v^2\lambda_a + w^2\lambda_b + \sqrt{\dots}$	
$c_\eta \text{Re}[(\tilde{l}_{\rm R}{}^2)_2] - s_\eta \text{Re}[\tilde{h}_2^2]$	$v^2\lambda_a + w^2\lambda_b - \sqrt{\dots}$	$\sim \mathcal{O}(v^2)$ for $\tan\alpha \sim 0$
$(\tilde{l}_{\rm R}{}^1)_2$	0	Global Goldstone
$\tilde{h}_2^1$	0	Gauge Goldstone
$\text{Im}[\tilde{h}_2^2]$	0	Gauge Goldstone
$\text{Im}[(\tilde{l}_{\rm R}{}^2)_2]$	0	Gauge Goldstone
$c_\alpha(\tilde{l}_{\rm R}{}^2)_1 + s_\alpha \tilde{h}_1^2$	0	Gauge Goldstone

Table 11. Case A: mass eigenstates in $\tilde{h}$ and $\tilde{l}_{\rm R}$ after SSB of the LR symmetry group to $\text{U}(1)_{\text{E.M.}}$ and the corresponding tree-level masses. Here, $\sqrt{\dots} = \sqrt{(v^2\lambda_a - w^2\lambda_b)^2 + (vw\lambda_f)^2}$, $c_\alpha = \cos\alpha$, $s_\alpha = \sin\alpha$ with $\tan\alpha = v/w$ and $c_\eta = \cos\eta$, $s_\eta = \sin\eta$ with η being the corresponding mixing angle whose explicit form we omit for simplicity.

Fields	$(\text{Mass})^2$	Comment
$c_\alpha \text{Re}[\tilde{h}_2^1] + s_\alpha \text{Re}[(\tilde{l}_{\rm R}{}^2)_1]$	$-\frac{1}{2}(v^2+w^2)\lambda_g$	
$s_\alpha \text{Im}[(\tilde{l}_{\rm R}{}^2)_1] - c_\alpha \text{Im}[\tilde{h}_2^1]$	$-\frac{1}{2}(v^2+w^2)\lambda_g$	
$(\tilde{l}_{\rm R}{}^1)_1$	$-\frac{1}{2}v^2\lambda_g + 2w^2\lambda_i$	
$\tilde{h}_2^2$	$-\frac{1}{2}w^2\lambda_g + 2v^2\lambda_j$	
$c_\kappa \text{Re}[\tilde{h}_1^1] + s_\kappa \text{Re}[(\tilde{l}_{\rm R}{}^2)_2]$	$v^2\lambda_a + w^2\lambda_b + \sqrt{\dots}$	
$c_\kappa \text{Re}[(\tilde{l}_{\rm R}{}^2)_2] - s_\kappa \text{Re}[\tilde{h}_1^1]$	$v^2\lambda_a + w^2\lambda_b - \sqrt{\dots}$	$\sim \mathcal{O}(v^2)$ for $\tan\alpha \sim 0$
$(\tilde{l}_{\rm R}{}^1)_2$	0	Global Goldstone
$\tilde{h}_1^2$	0	Gauge Goldstone
$\text{Im}[\tilde{h}_1^1]$	0	Gauge Goldstone
$\text{Im}[(\tilde{l}_{\rm R}{}^2)_2]$	0	Gauge Goldstone
$-s_\alpha \text{Re}[\tilde{h}_2^1] + c_\alpha \text{Re}[(\tilde{l}_{\rm R}{}^2)_1]$	0	Gauge Goldstone
$c_\alpha \text{Im}[(\tilde{l}_{\rm R}{}^2)_1] + s_\alpha \text{Im}[\tilde{h}_2^1]$	0	Gauge Goldstone

Table 12. Case B: mass eigenstates in $\tilde{h}$ and $\tilde{l}_{\rm R}$ after SSB of the LR symmetry group directly to $\text{U}(1)_{\text{E.M.}}$ and the corresponding tree-level masses. Here, $\sqrt{\dots} = \sqrt{(v^2\lambda_a - w^2\lambda_b)^2 + v^2w^2(\lambda_g - \lambda_f)^2}$, $c_\alpha = \cos\alpha$, $s_\alpha = \sin\alpha$ with $\tan\alpha = v/w$ and $c_\kappa = \cos\kappa$, $s_\kappa = \sin\kappa$ with κ being the corresponding mixing angle whose explicit form we omit for simplicity.

JHEP09(2016)129

6.1 Parameter scan

Effectively, we would like to explore a five-dimensional parameter subspace of the high-scale model $\{\lambda_3, \varepsilon, \delta, g, y\}$ assuming we have fixed the scale at which trinification is broken and imposed the constraints in eq. (3.6). This is due to the fact that in the effective LR-symmetric model after tree-level matching, the β-functions only depend on those parameters as seen in eq. (4.9). Once a consistent set of high-scale model parameters is found, the matching can be performed and the RG equations can be numerically integrated yielding a scale dependence of the effective model parameters. The running starts from the matching scale μ_m, which is chosen to be the trinification breaking VEV,

$$\mu_m = v_3, \tag{6.1}$$

since the heavy states in the trinification theory that we integrate out have masses of $\mathcal{O}(v_3)$. The running is then terminated at a lower scale μ_r, which is defined as

$$\mu_r = \sqrt{\frac{|m_R^2(\mu_r)| + |m_h^2(\mu_r)|}{2}}, \tag{6.2}$$

since, at this scale, there are again states with masses of the same order as the renormalisation scale. These states then have to be integrated out before we can run down even further. Depending on the initial values at a high scale, m_R^2 may have run negative at this scale, thus triggering the radiative symmetry breaking we are looking for. However, we have to guarantee that, at the stopping scale μ_r, the minimisation conditions for the VEV setting described in eq. (5.1) are satisfied (i.e. that all the squared masses in table 8 are positive).

6.1.1 Simulated annealing

In order to find viable parameter space points in the high-scale theory, we implemented the SA algorithm together with the numerical integration of β functions. The SA is a method for estimating the global minimum of a given function $E(\{p_i\})$ in a multi-dimensional parameter space $\{p_i\}$ [58].

If we interpret the function $E(\{p_i\})$ as the energy of a system whose physical state is defined by $\{p_i\}$, and imagine that the system is in thermal contact with a heat bath with temperature T, we can let this system approach its equilibrium state by employing the Metropolis algorithm. That is, we start with a random set of initial parameters, and propose random updates $\{p_i\} \to \{p'_j\}$ that are accepted with probability

$$P_{\text{acc}}(\{p_i\} \to \{p'_i\}) = \begin{cases} 1 & \text{if } E(\{p'_i\}) < E(\{p_i\}) \\ \mathrm{e}^{(E(\{p_i\}) - E(\{p'_i\}))/T} & \text{otherwise,} \end{cases} . \tag{6.3}$$

Given a constant T, this procedure fulfils detailed balance w.r.t. the canonical ensemble $\mathcal{P}(\{p_i\}) \propto \mathrm{e}^{-E(\{p_i\})/T}$, which in the limit $T \to \infty$ is a flat distribution where all $\{p_i\}$ are equally likely, while in the limit $T \to 0$ becomes highly peaked for the ground states of the system, i.e. the states $\{p_i\}$ that minimise $E(\{p_i\})$.

JHEP09(2016)129

The SA works by initialising the system at a large temperature, and then running the Metropolis algorithm while slowly (i.e. adiabatically) decreasing the temperature until $T \sim 0$. In this way, $E(\{p_i\})$ is minimised and the corresponding parameter space points $\{p_i\}$ are found. This procedure has the advantage of being easy to implement while also being less prone to get stuck in local minima compared to for example a gradient descent method since local energy barriers can be overcome by "thermal fluctuations".

For the purpose of this work we defined

$$E = \begin{cases} 10 & \text{if } m_R^2(\mu) > 0 \,\forall\, \mu \in (m_Z, \mu_m) \\ 5 + \frac{\min(m_i^2)}{\max(|m_i^2|)} & \text{if } m_j^2 < 0 \text{ for some } j \\ 2\frac{\min(m_{h_i}^2)}{\min(m_q^2, m_{Z'}^2, m_{W'}^2)} + \frac{\min(m_{h_i}^2)}{\max(m_q^2, m_{r_2}^2, m_{Z'}^2, m_{W'}^2)} & \text{if } m_R^2(\mu_r) < 0 \text{ and } m_j^2(\mu_r) > 0 \end{cases} \tag{6.4}$$

where $E = E(\lambda_3, \epsilon, \delta, g, y)$ and $m_i^2 = (m_q^2, m_{h_i}^2, m_{R_i}^2, m_{Z'}^2, m_{W'}^2)$ are the masses after radiative symmetry breaking evaluated at the scale μ_r. Minimisation of this function guarantees that we find parameter space points where m_R^2 runs negative while also introducing a bias towards parameters that yield a light Higgs-like $\mathrm{SU(2)_L}$ doublet.

6.1.2 Choosing the trinification breaking scale

One of the free parameters of the proposed framework is the scale at which trinification symmetry is spontaneously broken. This scale, which is the starting point for all the successive symmetry breakings at low scales, is defined only by the trinification breaking VEV (3.1). In order to get an idea of what scales are sensible to explore, we integrated the one-loop RG equations for gauge couplings in the effective LR-symmetric model, an easy task due to the fact that at one-loop the β-functions only depend on the gauge couplings themselves. It was possible then to relate the trinification breaking scale to the measured values of the SM $\mathrm{SU(2)_L}$, $\mathrm{U(1)_Y}$ and $\mathrm{SU(3)_C}$ gauge couplings. We found that for a trinification breaking scale of $\mu_m = 10^{12.2}$ GeV, the boundary condition of $g_0 = 0.61$ leads roughly to the SM values at m_Z. In figure 1 we show the result from integrating the gauge coupling β-functions from μ_m down to m_Z. Because the β-functions only depend on the gauge couplings at one-loop, this running is valid for any parameter space point with $g_0 = 0.61$ as boundary condition. We show in the same plot

$$g_Y(\mu) \equiv \frac{2\, g_R\, g_{L+R}}{\sqrt{4g_{L+R}^2 + g_R^2}} \tag{6.5}$$

which would be the matching condition for g_1, the hypercharge gauge coupling, as function of the scale μ. Note however that in figure 1, the running is performed all the way down to the EW scale m_Z, without decoupling the massive states at μ_r. A more accurate calculation would implement this intermediate step, which would alter the slopes of the lines in figure 1 at scales below μ_r. Therefore, this calculation should only serve as a very rough estimate of the numerical values of the matching scale (and the value of the trinification gauge coupling at this scale).

JHEP09(2016)129

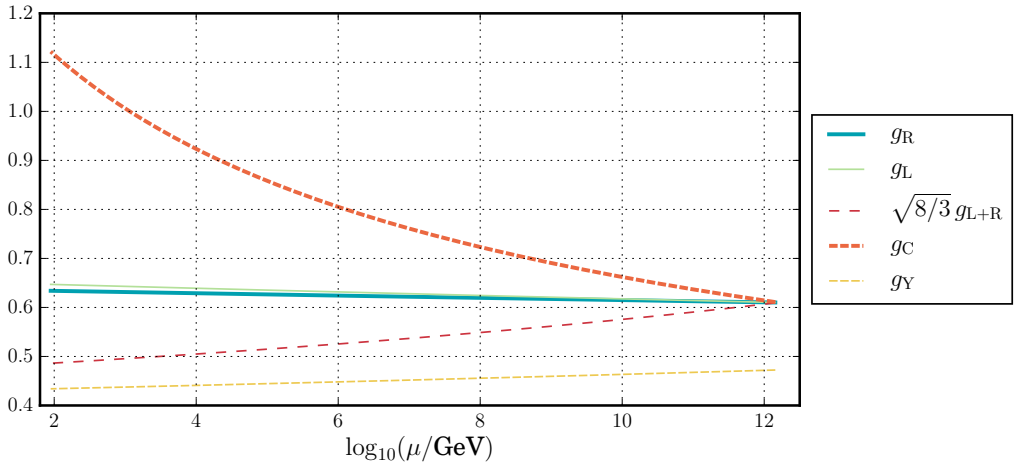

Figure 1. One-loop RG evolution of gauge couplings in the effective LR-symmetric model and matching condition for the hypercharge coupling g_Y with $g_0 = 0.61$. A trinification breaking scale of $\mu_m \approx 10^{12.2}$ GeV leads to roughly SM values for $g_\mathrm{L} \equiv g_2$, $g_\mathrm{C} \equiv g_3$ and $g_\mathrm{Y} \equiv g_1$ at $\mu \approx m_Z$.

6.2 Regions of parameter space with radiative breaking

Using the framework described above we found 22081 parameter space points by running our implementation of the SA algorithm allowing for high-scale parameters within the unitarity bounds and for a trinification breaking scale of $\mu_m = 10^{12.2}$ GeV. Remarkably, we found that the considered model naturally contains large parameter space regions where $\mathrm{SU}(2)_\mathrm{R} \times \mathrm{U}(1)_\mathrm{L+R}$ is radiatively broken down to $\mathrm{U}(1)_\mathrm{Y}$ while a light Higgs doublet remains in the spectrum at the stopping scale μ_r. In figure 2 we show the allowed regions in several slices of the high-scale parameter space. Most of the features of these regions can be explained by the structure of the mass-parameter β-functions in eqs. (A.13) and (A.12). Our algorithm selects points where m_R^2 would have a positive β-function so that it could run to negative values at low scales. For example, we see that the allowed parameter space region always satisfies $\epsilon < \delta$ which translates into the inequality $m_R^2 < m_h^2$ at the matching scale. Although one can find points for which (A.13) is positive and $\epsilon > \delta$, for such points m_h^2 value runs negative before m_R^2 does. This would trigger an unwanted simultaneous breaking of $\mathrm{SU}(2)_\mathrm{L}$ and $\mathrm{SU}(2)_\mathrm{R}$ with the same VEV, as opposed to the desired situation where the VEV responsible for $\mathrm{SU}(2)_\mathrm{R} \times \mathrm{U}(1)_\mathrm{L+R} \to \mathrm{U}(1)_\mathrm{Y}$ is much larger than the Higgs VEV that triggers the EW symmetry breaking.

We selected the most promising candidates from the results of the scan by requiring the maximal hierarchy between a light Higgs-like doublet and heavy exotic particles at the scale μ_r while having parameters within the perturbativity constraints. In figure 3 we show the running of mass parameters before and after the radiative $\mathrm{SU}(2)_\mathrm{R} \times \mathrm{U}(1)_\mathrm{L+R}$ symmetry breaking for a benchmark point satisfying those conditions. We find that it is possible to find some mass hierarchy at the symmetry breaking scale, with a Higgs-like scalar doublet coming from $\tilde{h}$ with masses up to two orders of magnitude lighter than the rest of the mass spectrum. In addition, we also observe that a complex scalar coming from $\tilde{l}_\mathrm{R}$ prefers to have a small mass at μ_r (this is the dark solid curve in figure 3, corresponding to $m_{r_2}^2$ in table 8). This scalar is a singlet under $\mathrm{SU}(2)_\mathrm{L}$ while having unit hypercharge, meaning that

JHEP09(2016)129

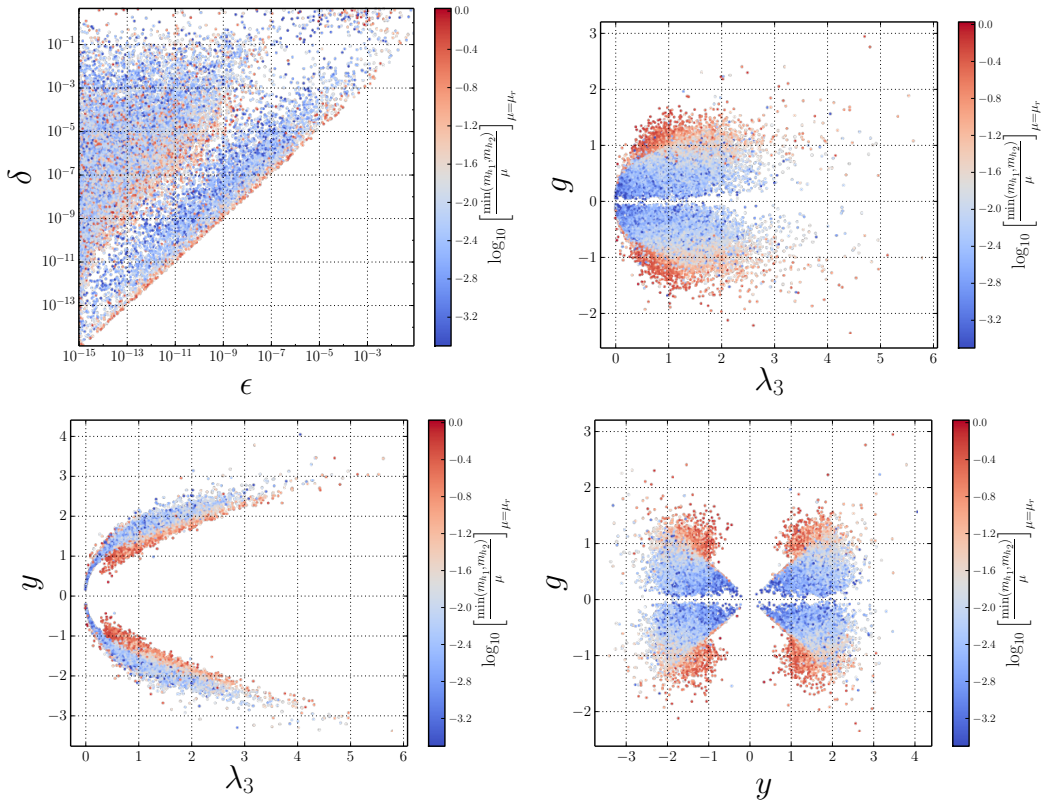

Figure 2. Regions of the high-scale model parameter space with the radiative $\mathrm{SU}(2)_\mathrm{R} \times \mathrm{U}(1)_\mathrm{L+R}$ symmetry breaking down to $\mathrm{U}(1)_\mathrm{Y}$ by RG evolution in the effective LR-symmetric model. The ranges for the scan were chosen such as to preserve the unitarity property at tree-level. The colours indicate the lightness of the lightest Higgs doublet compared to the renormalization scale at the stopping scale μ_r.

it will have unit electric charge after EW symmetry breaking. At present, it is not clear to what extent this state accumulates a much larger mass when evolving from μ_r down to the EW scale.

Although the gauge couplings of the effective LR-symmetric model start with the same values due to the matching conditions and the $\mathbb{Z}_3$ symmetry in the high-scale model, the RG evolution induces a splitting as seen in figure 1. It is interesting to note that although we did not impose the boundary condition $g_0 = 0.6$ for the SA algorithm, the allowed points in parameter space seem to be consistent with the boundary condition as seen in the upper right plot in figure 2. We also note from figure 1 that there is an approximate relation $g_\mathrm{L} \approx g_\mathrm{R}$ that is exact at the matching scale, while a small splitting between g_L and g_R is generated in the low energy limit. This observation points towards an approximate $\mathbb{Z}_2$ symmetry between the $\mathrm{SU}(2)_\mathrm{L}$ and $\mathrm{SU}(2)_\mathrm{R}$ gauge groups. In fact, we can trace the origin of the radiative $\mathbb{Z}_2$ breaking to the scalar sector in the effective model, where the choice of keeping only $\tilde{l}_\mathrm{R}$ and $\tilde{h}$ leads to $\beta_{g_\mathrm{L}} \neq \beta_{g_\mathrm{R}}$. This is because only $\tilde{h}$ transforms under $\mathrm{SU}(2)_\mathrm{L}$ (while both $\tilde{l}_\mathrm{R}$ and $\tilde{h}$ transform under $\mathrm{SU}(2)_\mathrm{R}$).

This serves to prove that in the proposed framework it is possible to trigger the full symmetry breaking down to the SM gauge group by means of the trinification breaking

JHEP09(2016)129

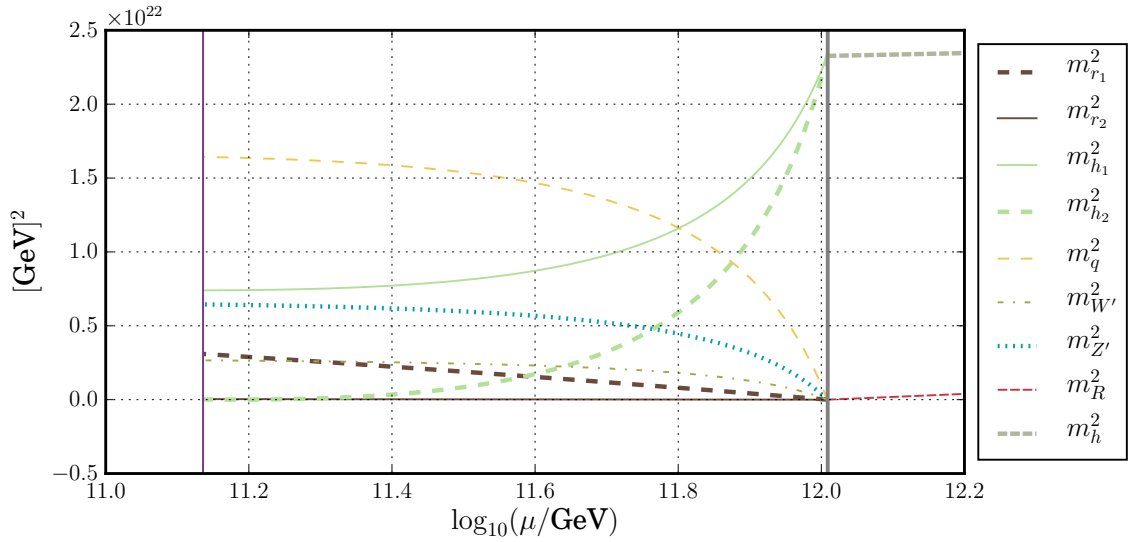

Figure 3. One-loop RG evolution of the mass parameters before and after the radiative $\mathrm{SU}(2)_\mathrm{R} \times \mathrm{U}(1)_\mathrm{L+R}$ symmetry breaking down to $\mathrm{U}(1)_\mathrm{Y}$ for an example point. The two vertical lines mark the scales at which m_R^2 first runs negative (right) and the scale μ_r at which the RG running is terminated (left), respectively.

VEV (3.1) only, while at the same time generating a desired hierarchy at low energy scales. In other words, in the model proposed in this work, the RG evolution makes it possible to have a highly symmetric trinification model whose gauge group is naturally broken down to the SM gauge group.

For the alternative case of breaking directly to $\mathrm{U}(1)_\mathrm{E.M.}$ discussed in section 5.2 we performed a similar analysis as we did above by preparing a SA scan to find parameter space points looking for a possibility for the radiative breaking to $\mathrm{U}(1)_\mathrm{E.M.}$. For case A (discussed in section 5.2.1) 6080 points were produced during three weeks where both m_h^2 and m_R^2 ran negative. However, none of the points showed positive squared masses in the scalar sector, i.e. no points were found where the desired vacuum was a minimum of the scalar potential. Similarly, for case B (discussed in section 5.2.2) we run a SA scan that produced 32631 points, again with none of them showing stable minima with the desired radiative symmetry breaking. What this means is that as far as our analysis could tell, when m_h^2 and m_R^2 became negative through RG running, the true minimum of the scalar potential did not exhibit $\mathrm{U}(1)_\mathrm{E.M.}$ as a remaining symmetry, thus making it unviable as a phenomenological model within the proposed framework.

7 Discussion and future work

7.1 Fermion sector at one-loop

In the present analysis, many Yukawa couplings (and also the Majorana mass m_{Φ^s}) in the effective LR-symmetric model are zero simply due to the tree-level matching procedure. However, this will no longer be true once the matching and running are performed at

JHEP09(2016)129

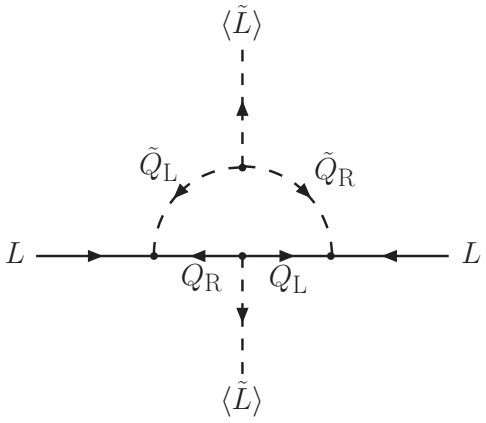

Figure 4. A diagram in the trinification theory that constitutes the one-loop contribution to the matching onto the Majorana Φ^s mass, m_{Φ^s}, in the effective LR-symmetric model.

a higher loop level. Although the full one-loop matching and two-loop running analysis is necessary to obtain precise numerical values that is planned for a future work, it is interesting to understand which diagrams will lead to non-vanishing matching conditions for some of the parameters in eq. (4.10).

We first note that m_{Φ^s} receives a non-zero contribution from the diagram in figure 4, with the trinification VEV in eq. (3.1). From this we can estimate that m_{Φ^s} will be suppressed with respect to the trinification breaking scale v_3 as

$$m_{\Phi^s}^{(1-\text{loop})} \sim \left(\frac{y^3}{(4\pi)^2}\cdot\frac{\gamma}{v_3}\right) v_3. \tag{7.1}$$

If the trinification Yukawa coupling y and the scalar tri-linear coupling γ are sufficiently large, it might be appropriate to integrate out Φ^s along with the heavy trinification-scale quarks in table 6, so that it no longer appears in the effective LR-symmetric model. If instead y and γ are small, the suppression factor in eq. (7.1) can easily be very small such that $m_{\Phi^s} \sim m_h, m_R$. At present, as was shown in section 6, we see no preference for neither large nor small values of y and γ, and both possibilities thus remain open.

Next, we turn to the Yukawa interactions that are generated by the diagrams in figure 5. These diagrams are of interest when the external leg $\tilde{L}$ corresponds to one of the two remaining scalars in the effective LR-symmetric model, namely $\tilde{h}$ and $\tilde{l}_{\rm R}$. One can then show that the diagram is non-vanishing when the external fermion legs are such that the loop corresponds to Yukawa interactions of the types

$$\begin{aligned}
&(\tilde{l}^*_{{\rm R}I})^R\ (l_{\rm R}{}^I)_R\,\Phi^s + \text{c.c.}\,,\\
&(\tilde{l}^*_{{\rm R}I})^R\ (l_{\rm R}{}^s)_R\,\Phi^I + \text{c.c.}\,,\\
&\tilde{h}^{*R}_L\ (l_{\rm L}{}^s)^L\,(l_{\rm R}{}^s)_R + \text{c.c.}\,,
\end{aligned} \tag{7.2}$$

i.e. the Yukawa couplings Y_γ, Y_δ and Y_η receive a non-zero contribution at one-loop. In particular, when $\langle\tilde{l}_{\rm R}\rangle \neq 0$ the upper two interaction terms in eq. (7.2) will provide masses

JHEP09(2016)129

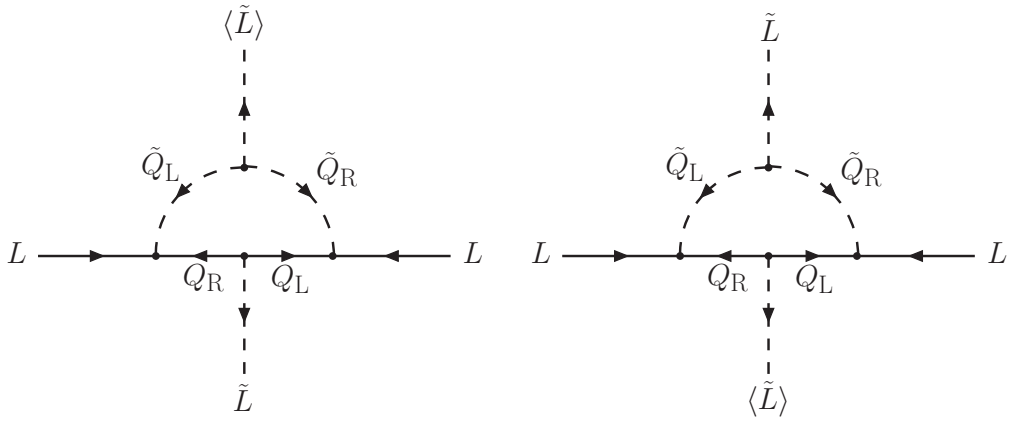

Figure 5. These two diagrams give rise to Yukawa terms that, in turn, provide Dirac masses for two generations of right-handed neutrinos and Φ's, as well as for SM leptons of the third generation.

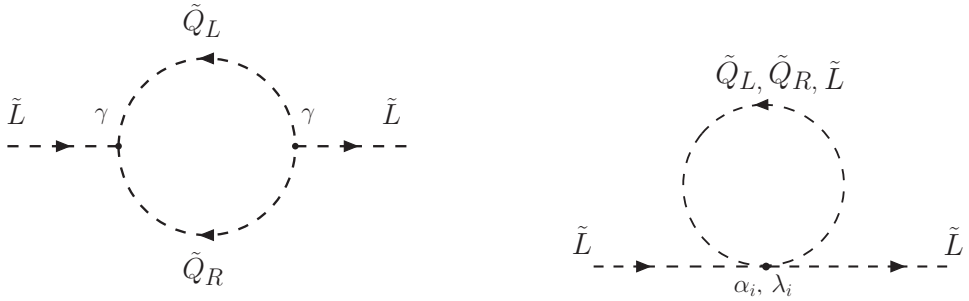

Figure 6. Class of diagrams with a non-vanishing contribution to m_h^2 and m_R^2 in the trinification theory.

to two generations of right-handed neutrinos. Note, however, that right-handed neutrinos receive a *Dirac* mass that is formed together with two generations of Φ. We can identify the last interaction term in eq. (7.2) as containing the Yukawa term for SM leptons of the third generation.

7.2 One-loop corrections to masses of light scalars

Although we have performed tree-level matching down to an effective theory, its important to understand whether the scalars $\tilde{h}_R^L$, $(\tilde{l}_{\rm R}{}^I)_R$ can remain light as soon as the higher-order corrections are considered. In general, this may not be the case and thus it would no longer be justified to keep those light scalars in the low-energy theory. Even if the corrections would keep the scalars sufficiently light, the particular values for their masses also affect the RG flow potentially leading to different conclusions regarding the radiative LR-symmetry breaking.

It turns out that the only non-vanishing one-loop contributions (in the zero external momenta approximation) to m_h^2 and m_R^2 come from the type of diagrams shown in figure 6. Any other topology will either (i) be forbidden by the trinification symmetry (such as fermion loops), or (ii) vanish once the zero momentum approximation is taken into account.

JHEP09(2016)129

The tri-linear coupling γ plays an important role in the one-loop matching conditions. Namely, it determines the size of the one-loop corrections to m_h^2 and m_R^2 coming from the left panel in figure 6. It thus suffices to make $\gamma/v_3 \ll 1$ in order to keep those corrections small.[3] For the second type of diagrams in figure 6 (right), the corrections become functions of λ_i but also α_i (the tree-level masses are only functions of λ_i). As long as the coloured scalars remain heavy, choosing appropriate values for α_i would give us enough freedom for $\tilde{h}_R^L$, $(\tilde{l}_{\rm R}{}^I)_R$ to remain light.

In the tree-level study of the model that has been presented here, we thus assume that the scalars are light leaving the specifics of the physical mechanism which appropriately tunes the values for γ and α_i as well as the corresponding effect on the RG evolution for future work. However, we expect that the qualitative conclusions reached in this work would still be valid when accounting for the higher-order corrections due to the fact that, as discussed in section 6, the regions of the effective theory parameter space where the radiative LR-symmetry breaking takes place are quite broad.

7.3 The low-energy LR-symmetric model with additional light Higgs-doublets

We have shown that the proposed model brings an intriguing possibility of the radiative $\mathrm{SU(2)_R \times U(1)_{L+R} \to U(1)_Y}$ breaking. To do this, we integrated out the maximal number of fields in the high scale trinification theory in order to make the effective LR-symmetric model as simple as possible. Although the radiative symmetry breaking in such a toy model is realized, we show in this section that in order to accurately generate all fermion masses in the SM, we need to consider the case where more scalars are present in the effective theory. This is due to the fact that some mass terms are forbidden by the global group that remains unbroken in the scenario considered in section 4. However, we note that the interplay between scalar mass parameters and their β-functions allowing m_R^2 to run negative, will still be present when integrating out fewer Higgs doublets. Although a more detailed study will be needed to find explicit regions of parameter space with the radiative symmetry breaking, we expect that the qualitative conclusions in section 6 will not be changed.

7.3.1 SM quarks

With tree-level matching (and one-loop running) the only non-zero Yukawa coupling with SM particles is Y_ζ in eq. (4.10). Arranging the $\tilde{h}$ and $\tilde{l}_{\rm R}$ VEVs as in eq. (5.9), we see that, through this term, v_1 gives masses to two up-type quarks which could be identified with the top and charm quarks of the SM. On the other hand, the VEV v_2 gives a mass to one down-type quark (which can be identified with the bottom quark) and also a contribution to the mass of the heavy down-type quark in table 10. However, there still remain one up-type and two down-type quarks that are massless at tree-level, which should be identified with the lightest *u, d, s* quarks in the SM. The corresponding left-handed and right-handed components are shown in table 13 along with their charges under the global group $\{\mathrm{U(1)_E \times U(1)_G}\}$, which is unbroken by the Higgs VEVs in eq. (5.9). Since none of the $Q_{\rm L}$ fields have

[3] The model presented here, while inspired by SUSY, is not supersymmetric. However, as long as SUSY is concerned, $\gamma/v_3 \ll 1$ condition could be justified by γ corresponding to a soft-SUSY breaking term whose natural values are around the SUSY breaking scale.

JHEP09(2016)129

Trinification	effective LR-symmetric model	$\mathrm{U}(1)_\mathrm{E}$	$\mathrm{U}(1)_\mathrm{G}$
$({Q_\mathrm{L}}^2)^c_2$	$({\mathcal{Q}_\mathrm{L}}^2)^c_2$	$-1/2$	$-1/6$
$({Q_\mathrm{L}}^3)^c_1$	$({\mathcal{Q}_\mathrm{L}}^s)^c_1$	$-1/2$	$-2/3$
$({Q_\mathrm{L}}^3)^c_2$	$({\mathcal{Q}_\mathrm{L}}^s)^c_2$	$-1/2$	$-2/3$
$(Q^\dagger_{\mathrm{R}3})^c_1$	$({\mathcal{Q}^\dagger_\mathrm{R}}^s)^1_c$	$+1/2$	$+1/3$
$(Q^\dagger_{\mathrm{R}3})^c_2$	$({\mathcal{Q}^\dagger_\mathrm{R}}^s)^2_c$	$+1/2$	$+1/3$
$(Q^\dagger_{\mathrm{R}3})^c_3$	$({D^\dagger_\mathrm{R}}^s)^3{}_c$	$+1/2$	$+5/6$

Table 13. Components in the trinification quark tri-triplets (and the corresponding fields in the effective LR-symmetric model) that should build up the left- and right-handed components of the lightest SM *u*, *d*, *s* quarks. In the current realisation of the model, the mass terms for these quarks are forbidden by the global $\{\mathrm{U}(1)_\mathrm{E} \times \mathrm{U}(1)_\mathrm{G}\}$ group that is left unbroken by the two Higgs VEVs.

the same global U(1) charges as any of the $Q^\dagger_\mathrm{R}$ fields in table 13, it is not possible to generate Dirac masses for the *u, d, s* quarks since those mass terms would violate $\{\mathrm{U}(1)_\mathrm{E} \times \mathrm{U}(1)_\mathrm{G}\}$. However, there is a simple way to accommodate these masses. For regions of parameter space with light Higgs doublets in the effective LR-symmetric model, their VEVs would break $\{\mathrm{U}(1)_\mathrm{E} \times \mathrm{U}(1)_\mathrm{G}\}$ enabling the radiative generation of the light quark mass terms.

7.3.2 Colour singlet fermions

As in the quark sector, many colour neutral fermion mass terms are forbidden by the global group that is left unbroken by the two Higgs VEVs. By looking at the global U(1) charges of the components of the colour neutral fermions, we find that the only electrically charged and electrically neutral fermions that can participate in a fermion bilinear term are contained in

$$\begin{aligned}
\psi_\mathrm{C} &= \Big(\; ({l_\mathrm{R}}^s)_1 \;\; ({l_\mathrm{L}}^s)^1 \;\; (H^2)^1_2 \;\Big|\; (H^s)^1_2 \;\; (H^s)^2_1 \;\; ({l_\mathrm{R}}^2)_1 \; \Big)^T , \\
\psi_\mathrm{N} &= \Big(\; ({l_\mathrm{R}}^s)_2 \;\; (H^2)^1_1 \;\; (H^2)^2_2 \;\; \Phi^2 \;\; ({l_\mathrm{L}}^s)^2 \;\Big|\; ({l_\mathrm{R}}^2)_2 \;\; (H^s)^1_1 \;\; (H^s)^2_2 \;\; \Phi^s \; \Big)^T ,
\end{aligned} \tag{7.3}$$

respectively. For all other colour neutral fermions, there is no fermion field with opposite U(1) charges such that they together could form a mass term. In particular, note that $\psi_{\mathrm{C,N}}$ contain no first generation colour singlet fermions.

Generally, we can then write the mass terms for the colour neutral fermions as

$$\frac{1}{2}\psi_\mathrm{C}^T M_\mathrm{C} \psi_\mathrm{C} + \frac{1}{2}\psi_\mathrm{N}^T M_\mathrm{N} \psi_\mathrm{N} + \text{c.c.} \tag{7.4}$$

Upon demanding invariance under the global U(1) groups (and of course $\mathrm{U}(1)_\mathrm{E.M.}$), we

JHEP09(2016)129

find that the mass matrices $M_{\mathrm{C,N}}$ have the following structure:

$$M_{\mathrm{C}} = \begin{pmatrix} \bullet & \bullet & & \\ \bullet & & & \\ \bullet & & & \\ & & & \bullet \\ & & & \bullet \\ & & \bullet & \end{pmatrix}, \qquad M_{\mathrm{N}} = \begin{pmatrix} \bullet & \bullet & \bullet & \bullet & & & & \\ \bullet & & & & & & & \\ \bullet & & & & & & & \\ \bullet & & & & & & & \\ & & & & \star & \bullet & \bullet & \bullet \\ & & & & \bullet & \star & \bullet & \bullet \\ & & & & \bullet & \bullet & \star & \bullet \\ & & & & \bullet & \bullet & \bullet & \star \end{pmatrix}, \tag{7.5}$$

where entries marked with a '$\bullet$' ('$\star$') denote the Dirac (Majorana) contributions that are allowed to be non-zero. These would amount to two electrically charged massive Dirac fermions (which we would have to identify with the τ-lepton and muon in the SM), one massive electrically neutral Dirac fermion, and four electrically neutral Weyl fermions that receive both Dirac and Majorana mass contributions.

The tri-triplet $(L^i)^l_r$ contains twelve electrically charged Weyl fermions, meaning that we will still have eight electrically charged Weyl fermions whose mass terms are forbidden by the unbroken global group. Out of the remaining fifteen electrically neutral components in $(L^i)^l_r$, at least nine Weyl fermions are necessarily massless. To make more components in $(L^i)^l_r$ massive (to evade obvious inconsistencies with phenomenology), we have to include more Higgs doublets in the effective LR-symmetric model originating from the high-scale trinification theory.

7.4 CKM mixing with additional Higgs doublets

In the previous section, we have seen that in order to explain the observed fermionic mass spectra, more components of $\tilde{L}$ should be kept in the effective LR-symmetric model. By looking at the CSS mass spectra, we see that this will be possible when

$$\lambda_{2,3,4} \ll \lambda_1 \,, \tag{7.6}$$

in which case the fields

$$(\tilde{L}^I)^L_R \,, \quad (\tilde{L}^I)^3_R \,, \quad (\tilde{L}^I)^L_3 \,, \quad (\tilde{L}^3)^L_R \,, \tag{7.7}$$

would all remain in the effective LR-symmetric model (see table 3). In this case, the CSS potential exhibits an approximate O(54) symmetry. Although this increase in the number of scalar fields would lead to a substantial increase in complexity in the low-energy theory, we are confident that the radiative $\mathrm{SU(2)_R \times U(1)_{L+R} \to U(1)_Y}$ breaking will still be present as mentioned above. In this section, we show in a straightforward tree-level analysis, that the structure of the SM Cabibbo-Kobayashi-Maskawa (CKM) mixing matrix in the Cabibbo form emerges as a consequence of $\mathrm{SU(3)_F}$ if VEVs are strategically placed

JHEP09(2016)129

in the tri-doublet $(\tilde{L}^I)^L_R$. These VEVs would be allowed at lower scales when keeping the extra fields in the effective theory after SSB of trinification.

Consider the following VEV setting:

$$\langle(\tilde{L}^1)^L_R\rangle = \frac{1}{\sqrt{2}}\begin{pmatrix} h_1 & 0 \\ 0 & h_2 \end{pmatrix}, \quad \langle(\tilde{L}^2)^L_R\rangle = \frac{1}{\sqrt{2}}\begin{pmatrix} h_3 & 0 \\ 0 & 0 \end{pmatrix} \tag{7.8}$$

In terms of the full trinification tri-triplet $\tilde{L}$, this means that

$$\langle\tilde{L}^1\rangle = \frac{1}{\sqrt{2}}\begin{pmatrix} h_1 & 0 & 0 \\ 0 & h_2 & 0 \\ 0 & 0 & 0 \end{pmatrix}, \qquad \langle\tilde{L}^2\rangle = \frac{1}{\sqrt{2}}\begin{pmatrix} h_3 & 0 & 0 \\ 0 & 0 & 0 \\ 0 & w & 0 \end{pmatrix}, \qquad \langle\tilde{L}^3\rangle = \frac{1}{\sqrt{2}}\begin{pmatrix} 0 & 0 & 0 \\ 0 & 0 & 0 \\ 0 & 0 & v_3 \end{pmatrix}. \tag{7.9}$$

where we have also indicated the trinification and LR symmetry breaking VEVs v_3 and w. The VEV setting (7.9) leaves the group

$$\mathrm{SU}(3)_\mathrm{C} \times \mathrm{U}(1)_\mathrm{E.M.} \times \{\mathrm{U}(1)_\mathrm{P} \times \mathrm{U}(1)_\mathrm{B}\} \tag{7.10}$$

unbroken, where the global $\mathrm{U}(1)_\mathrm{P}$ is generated by

$$T_\mathrm{P} \equiv \frac{1}{\sqrt{3}}\left(T^8_\mathrm{R} + T^8_\mathrm{F}\right). \tag{7.11}$$

For a consistency with the SM, we have to impose the following hierarchy between the above VEVs

$$v \gg w \gg h_{1,2,3} \sim 10^2 - 10^3\,\mathrm{GeV}, \tag{7.12}$$

such that $h_{1,2,3}$ would correspond to the SM-breaking Higgs VEVs. In the gauge sector, at tree level one recovers one massless (photon) state

$$A_\mu = \frac{1}{2\sqrt{2}}\left[G_{\mathrm{L}\mu}^{\ 8} + G_{\mathrm{R}\mu}^{\ 8} - \sqrt{3}(G_{\mathrm{L}\mu}^{\ 3} + G_{\mathrm{R}\mu}^{\ 3})\right], \tag{7.13}$$

$W^\pm$ bosons

$$W^\pm_\mu = G_{\mathrm{L}\mu}^{\ 1,2}, \qquad m^2_W \simeq \frac{1}{8}\,g^2\sum_i h_i^2, \tag{7.14}$$

and the Z^0 boson

$$Z^0_\mu = \frac{1}{2\sqrt{10}}\left[5G_{\mathrm{L}\mu}^{\ 3} - 3G_{\mathrm{R}\mu}^{\ 3} + \sqrt{3}(G_{\mathrm{L}\mu}^{\ 8} + G_{\mathrm{R}\mu}^{\ 8})\right], \qquad m^2_Z \simeq \frac{2}{10}\,g^2\sum_i h_i^2, \tag{7.15}$$

in a rough consistency with the SM. Besides, at w scale one finds heavy $W'^\pm$ and Z'^0 bosons

$$W'^\pm_\mu = G_{\mathrm{R}\mu}^{\ 1,2}, \qquad m^2_{W'} \simeq \frac{1}{8}\,g^2w^2, \tag{7.16}$$

$$Z'^0_\mu = \frac{1}{\sqrt{10}}\left[2G_{\mathrm{R}\mu}^{\ 3} + \sqrt{3}(G_{\mathrm{L}\mu}^{\ 8} + G_{\mathrm{R}\mu}^{\ 8})\right], \qquad m^2_{Z'} \simeq \frac{5}{16}\,g^2w^2, \tag{7.17}$$

JHEP09(2016)129

which can be recognised as the heavy vector states in table 9. The other nine gauge bosons corresponding to broken (by v_3) generators of $[\mathrm{SU}(3)]^2 \to [\mathrm{SU}(2)]^2$ in trinification get masses at the GUT scale $\mu_m \sim v_3$ (see table 9).

In the quark sector with $Q^i_{\mathrm{L}} = \{u^i_{\mathrm{L}}, d^i_{\mathrm{L}}, D^i_{\mathrm{L}}\}$, we obtain three weak-singlet down-type quarks $D^i = \{D, S, B\}$ that acquire large (Dirac) tree-level masses

$$m_B \simeq \frac{1}{\sqrt{2}} yw\,, \qquad m_D \simeq m_S \simeq \frac{1}{\sqrt{2}} yv\,, \tag{7.18}$$

and hence decouple from the SM. The other three down-type states $d^i = \{d, s, b\}$ remain light

$$m_d = 0\,, \qquad m_s \simeq m_b \simeq \frac{1}{\sqrt{2}} yh_2\,, \tag{7.19}$$

and could thus be identified with masses of down, strange and bottom quarks of the SM, respectively, such that there is no tree-level splitting between s and b quarks, and d-quark is massless. Interestingly enough, all the down-type quarks d^i and D^i practically do not mix with each other to the leading order in small h_i/v, h_i/w and w/v ratios. Note, while it is possible to introduce a non-zero tree-level splitting between s and b quarks by imposing more VEVs in neutral components of two Higgs doublets, a non-zero d-quark mass can only acquire a non-zero value by an unnaturally small VEV in a neutral component of a third Higgs doublet, but we do not consider this situation here. All the physical up-type quarks emerge as mixures of trinification up-type quarks $u^i = \{u^1, u^2, u^3\}$ remain light

$$u = \frac{u^1 h_1 + u^2 h_3}{\sqrt{h_1^2 + h_3^2}}\,, \qquad c = \frac{-u^2 h_1 + u^1 h_3}{\sqrt{h_1^2 + h_3^2}}\,, \qquad t = u^3\,, \tag{7.20}$$

$$m_u = 0\,, \qquad m_c \simeq m_t \simeq \frac{1}{\sqrt{2}} y \sqrt{h_1^2 + h_3^2}\,, \tag{7.21}$$

which could be identified with masses of up u, charm c and top t quarks of the SM, respectively. Again, in the considering scenario, there is no tree-level splitting between c and t, and it can not be generated at tree level by imposing any additional VEVs. The observed substantial charm-top and strange-bottom splittings can be in principle generated radiatively by (i) RG runnings of the corresponding Yukawa couplings which will have different slopes as long as trinification symmetry is broken, and by (ii) higher-loop effects which may modify the starting values for the Yukawa couplings at the matching scale. The quark CKM mixing aquires an approximate Cabbibo form already at tree level

$$V^{\mathrm{CKM}} \simeq \begin{pmatrix} \cos\theta_C & \sin\theta_C & 0 \\ -\sin\theta_C & \cos\theta_C & 0 \\ 0 & 0 & 1 \end{pmatrix}\,, \qquad \tan\theta_C = \frac{h_1}{h_3}\,, \tag{7.22}$$

which is a remarkable feature of the family symmetry, while small observed distortions of the Cabbibo mixing could only be generated at a higher-loop level. Non-unitarity corrections to the quark CKM mixing are also suppressed by small h_i/v, h_i/w and w/v ratios. This means that phenomenological constraints on those corrections could be important for setting lower limits on hierarchies between the trinification symmetry breaking scales.

JHEP09(2016)129

8 Conclusions

In this work we have introduced a GUT based on the trinification gauge group. By introducing a global $SU(3)_F$ family symmetry, our model resolves some of the issues with previous attempts to work with gauge trinification-based models while also considerably reduces the number of free parameters.

We found that SSB of the trinification symmetry can be triggered by the VEV of only one component of a scalar **27**-plet and that the minimum is, in a large part of the parameter space, the global one. We found that radiative breaking of gauge (i.e. $SU(2)_R \times U(1)_{L+R}$) and global symmetries, that are not present in the SM, was possible in the effective LR-symmetric model that is left after SSB of trinification. We did so by studying the most simple scenario (two light scalar multiplets remaining in the effective theory) where the mass-squared parameter for a scalar field charged under such symmetries could become negative by means of the RG evolution. By implementing a parameter scan algorithm using simulated annealing, we were able to efficiently scan the parameter space of the trinification theory and found regions where the radiative breaking happens in the chosen effective LR-symmetric model.

We also explored under which circumstances the high-scale theory might reproduce the masses and hierarchies of the SM at lower energies. We found that the simple scenario used to understand the radiative symmetry breaking needs to be extended in order to get for example CKM mixing and masses for all SM fermions. By having more light scalar multiplets present in the effective theory, their VEVs could break the remaining global symmetries which forbid the necessary mass terms in the low-energy theory. We also show that if such fields are present, the proposed model has good potential to result in a realistic quark mass spectrum resembling the SM one, while keeping the ingredients necessary to trigger the radiative breaking shown in this work. It is clear then that future studies should include one-loop matching, two-loop RG running and the extra scalar multiplets in the effective theory. Although we have shown the feasibility of radiative breaking and the possibility to explain the hierarchies in mass parameters for the proposed model, in order to offer a complete consistency with the SM such extended study needs to be performed in future work.

Acknowledgments

The authors would like to thank N.-E. Bomark, E. Corrigan, W. Porod, M. Sampaio and F. Staub for insightful discussions during the development of this work. A. P. M. is supported by the FCT grant SFRH/BPD/97126/2013 and partially by the H2020-MSCA-RISE-2015 Grant agreement No StronGrHEP-690904, and by the CIDMA project UID/MAT/04106/2013. A. P. M. also acknowledges the THEP group at Lund University for all hospitality and significant support provided for the development of this work. J. E. C.-M., R. P. and J. W. acknowledge the warm hospitality of the Gr@v group at Aveiro University. The work by J. E. C.-M. was supported by the Crafoord Foundation. R. P. and J. W. were partially supported by the Swedish Research Council, contract number 621-2013-428.

JHEP09(2016)129

A RG equations for the LR-symmetric theory

In this appendix we list the one-loop β-functions for the LR symmetric theory described in section 4. The convention we will follow is that for a given coupling g, the βfunction is defined as

$$\beta_g = \frac{\mathrm{d}g}{\mathrm{d}t} \tag{A.1}$$

where $t = \log(\mu)$ with μ the renormalisation scale.

A.1 Gauge couplings

$$(4\pi)^2\beta_{g_\mathrm{R}} = -\frac{2}{3}g_\mathrm{R}^3 \tag{A.2}$$

$$(4\pi)^2\beta_{g_\mathrm{L}} = -g_\mathrm{L}^3 \tag{A.3}$$

$$(4\pi)^2\beta_{g_{\mathrm{L+R}}} = \frac{124}{9}g_{\mathrm{L+R}}^3 \tag{A.4}$$

$$(4\pi)^2\beta_{g_\mathrm{C}} = -\frac{19}{3}g_\mathrm{C}^3 \tag{A.5}$$

A.2 Yukawa couplings

$$(4\pi)^2\beta_{Y_\alpha} = \left(\frac{7}{2}|Y_\alpha|^2 + |Y_\beta|^2 + 3|Y_\gamma|^2 + 2|Y_\delta|^2 - \frac{9}{4}g_\mathrm{R}^2 - 3g_{\mathrm{L+R}}^2\right) Y_\alpha \tag{A.6}$$

$$(4\pi)^2\beta_{Y_\beta} = \left(|Y_\alpha|^2 + 3|Y_\beta|^2 + 3|Y_\gamma|^2 + |Y_\epsilon|^2 - \frac{9}{4}g_\mathrm{R}^2 - 3g_{\mathrm{L+R}}^2\right) Y_\beta \tag{A.7}$$

$$(4\pi)^2\beta_{Y_\gamma} = \left(|Y_\alpha|^2 + |Y_\beta|^2 + \frac{11}{2}|Y_\gamma|^2 + |Y_\zeta|^2 - 8g_\mathrm{C}^2 - \frac{9}{4}g_\mathrm{R}^2 - \frac{5}{3}g_{\mathrm{L+R}}^2\right) Y_\gamma \tag{A.8}$$

$$(4\pi)^2\beta_{Y_\delta} = \left(2|Y_\alpha|^2 + \frac{7}{2}|Y_\delta|^2 + |Y_\epsilon|^2 + 6|Y_\zeta|^2 - \frac{9}{4}g_\mathrm{L}^2 - \frac{9}{4}g_\mathrm{R}^2\right) Y_\delta \tag{A.9}$$

$$(4\pi)^2\beta_{Y_\epsilon} = \left(|Y_\beta|^2 + |Y_\delta|^2 + 3|Y_\epsilon|^2 + 6|Y_\zeta|^2 - \frac{9}{4}g_\mathrm{L}^2 - \frac{9}{4}g_\mathrm{R}^2 - 6g_{\mathrm{L+R}}^2\right) Y_\epsilon \tag{A.10}$$

$$(4\pi)^2\beta_{Y_\zeta} = \left(\frac{1}{2}|Y_\gamma|^2 + |Y_\delta|^2 + |Y_\epsilon|^2 + 8|Y_\zeta|^2 - 8g_\mathrm{C}^2 - \frac{9}{4}g_\mathrm{L}^2 - \frac{9}{4}g_\mathrm{R}^2 - \frac{2}{3}g_{\mathrm{L+R}}^2\right) Y_\zeta \tag{A.11}$$

A.3 Scalar masses

$$\begin{aligned}(4\pi)^2\beta_{m_h^2} = &\left(20\lambda_a - 8\lambda_j + 2|Y_\delta|^2 + 2|Y_\epsilon|^2 + 12|Y_\zeta|^2 - \frac{9}{2}g_\mathrm{L}^2 - \frac{9}{2}g_\mathrm{R}^2\right) m_h^2 \\ &+ 4\left(\lambda_g + 2\lambda_f\right) m_R^2 - 4|Y_\delta|^2 m_{\Phi^s}^2\end{aligned} \tag{A.12}$$

$$\begin{aligned}(4\pi)^2\beta_{m_R^2} = &\left(20\lambda_b - 8\lambda_i + 2|Y_\alpha|^2 + 2|Y_\beta|^2 + 6|Y_\gamma|^2 - \frac{9}{2}g_\mathrm{R}^2 - 6g_{\mathrm{L+R}}^2\right) m_R^2 \\ &+ 4\left(\lambda_g + 2\lambda_f\right) m_h^2 - 4|Y_\alpha|^2 m_{\Phi^s}^2\end{aligned} \tag{A.13}$$

A.4 Singlet Fermion mass

$$(4\pi)^2\beta_{m_{\Phi^s}} = 4(|Y_\alpha|^2 + |Y_\delta|^2)m_{\Phi^s} \tag{A.14}$$

JHEP09(2016)129

A.5 Quartic couplings

$$
\begin{aligned}
(4\pi)^2\beta_{\lambda_a} &= 32\lambda_a^2 + 4\lambda_f^2 + 2\lambda_g^2 + 4\lambda_f\lambda_g + 16\lambda_j^2 - 16\lambda_a\lambda_j + 4\left(|Y_\epsilon|^2 + |Y_\delta|^2 + 6|Y_\zeta|^2\right)\lambda_a \\
&\quad - 2\left(|Y_\epsilon|^4 + |Y_\delta|^4 + 6|Y_\zeta|^4\right) - 9\left(g_{\mathrm{L}}^2 + g_{\mathrm{R}}^2\right)\lambda_a + \frac{9}{8}g_{\mathrm{L}}^4 + \frac{3}{4}g_{\mathrm{L}}^2 g_{\mathrm{R}}^2 + \frac{9}{8}g_{\mathrm{R}}^4 \qquad \text{(A.15)} \\
(4\pi)^2\beta_{\lambda_b} &= 32\lambda_b^2 + 4\lambda_f^2 + 2\lambda_g^2 + 4\lambda_f\lambda_g + 16\lambda_i^2 - 16\lambda_b\lambda_i + 4\left(|Y_\alpha|^2 + |Y_\beta|^2 + 3|Y_\gamma|^2\right)\lambda_b \\
&\quad - 2\left(|Y_\alpha|^4 + |Y_\beta|^4 + 3|Y_\gamma|^4\right) - 3\left(3g_{\mathrm{R}}^2 + 4g_{\mathrm{L+R}}^2\right)\lambda_b \\
&\quad + \frac{9}{8}g_{\mathrm{R}}^4 + 3g_{\mathrm{R}}^2 g_{\mathrm{L+R}}^2 + 6g_{\mathrm{L+R}}^4 \qquad \text{(A.16)} \\
(4\pi)^2\beta_{\lambda_f} &= 4\lambda_f^2 + 2\lambda_g^2 + 4\left(5\lambda_f + 2\lambda_g\right)\left(\lambda_a + \lambda_b\right) - 8\left(\lambda_f + \lambda_g\right)\left(\lambda_i + \lambda_j\right) \\
&\quad + 2\left(|Y_\alpha|^2 + |Y_\beta|^2 + 3|Y_\gamma|^2 + |Y_\delta|^2 + |Y_\epsilon|^2 + 6|Y_\zeta|^2\right)\lambda_f \\
&\quad - 4\left(|Y_\alpha|^2|Y_\delta|^2 + |Y_\beta|^2|Y_\epsilon|^2 + 3|Y_\gamma|^2|Y_\zeta|^2\right) \\
&\quad - 3\left(\frac{3}{2}g_{\mathrm{L}}^2 + 3g_{\mathrm{R}}^2 + 2g_{\mathrm{L+R}}^2\right)\lambda_f + \frac{9}{4}g_{\mathrm{R}}^4 \qquad \text{(A.17)} \\
(4\pi)^2\beta_{\lambda_g} &= \lambda_g(2|Y_\alpha|^2 + 2|Y_\beta|^2 + 6|Y_\gamma|^2 + 2|Y_\delta|^2 + 2|Y_\epsilon|^2 + 12|Y_\zeta|^2) \\
&\quad - \frac{9}{2}\lambda_g g_{\mathrm{L}}^2 + \frac{1}{2}|Y_\alpha|^2|Y_\delta|^2 + \frac{5}{2}|Y_\beta|^2|Y_\epsilon|^2 + \frac{15}{2}|Y_\gamma|^2|Y_\zeta|^2 \\
&\quad + 8\lambda_g\lambda_i + 8\lambda_g\lambda_j + 8\lambda_f\lambda_g + 4\lambda_b\lambda_g + 4\lambda_a\lambda_g - 9\lambda_g g_{\mathrm{R}}^2 - 6\lambda_g g_{\mathrm{L+R}}^2 + 4\lambda_g^2 \qquad \text{(A.18)} \\
(4\pi)^2\beta_{\lambda_i} &= -16\lambda_i^2 + \lambda_g^2 + 24\lambda_b\lambda_i + 4\left(|Y_\alpha|^2 + 3|Y_\beta|^2 + 3|Y_\gamma|^2\right)\lambda_i \\
&\quad - \frac{1}{8}\left(|Y_\alpha|^4 + 5|Y_\beta|^4 + 3|Y_\gamma|^4\right) - 3\left(3g_{\mathrm{R}}^2 + 4g_{\mathrm{L+R}}^2\right)\lambda_i + 3g_{\mathrm{L+R}}^2 g_{\mathrm{R}}^2 \qquad \text{(A.19)} \\
(4\pi)^2\beta_{\lambda_j} &= -16\lambda_j^2 + \lambda_g^2 + 24\lambda_a\lambda_j + 4\left(|Y_\delta|^2 + |Y_\epsilon|^2 + 6|Y_\zeta|^2\right)\lambda_j \\
&\quad - \frac{5}{8}\left(|Y_\delta|^4 + |Y_\epsilon|^4 + 6|Y_\zeta|^4\right) - 9\left(g_{\mathrm{R}}^2 + g_{\mathrm{L}}^2\right)\lambda_j - \frac{3}{2}g_{\mathrm{L}}^2 g_{\mathrm{R}}^2 \qquad \text{(A.20)}
\end{aligned}
$$

References

[1] ATLAS collaboration, *Observation of a new particle in the search for the Standard Model Higgs boson with the ATLAS detector at the LHC*, *Phys. Lett.* **B 716** (2012) 1 [arXiv:1207.7214] [INSPIRE].

[2] CMS collaboration, *Observation of a new boson at a mass of* 125 *GeV with the CMS experiment at the LHC*, *Phys. Lett.* **B 716** (2012) 30 [arXiv:1207.7235] [INSPIRE].

[3] A. De Rújula, H. Georgi and S.L. Glashow, *Trinification of all elementary particle forces*, in *Fifth Workshop on Grand Unification*, K. Kang, H. Fried and F. Frampton eds., World Scientific, Singapore (1984).

[4] K.S. Babu, X.-G. He and S. Pakvasa, *Neutrino masses and proton decay modes in* SU(3) × SU(3) × SU(3) *trinification*, *Phys. Rev.* **D 33** (1986) 763 [INSPIRE].

[5] G. Lazarides and C. Panagiotakopoulos, *MSSM from SUSY trinification*, *Phys. Lett.* **B 336** (1994) 190 [hep-ph/9403317] [INSPIRE].

JHEP09(2016)129

[6] G. Lazarides and C. Panagiotakopoulos, *MSSM and large* $\tan\beta$ *from SUSY trinification*, *Phys. Rev.* **D 51** (1995) 2486 [hep-ph/9407286] [INSPIRE].

[7] J.E. Kim, Z_3 *orbifold construction of* $\mathrm{SU}(3)^3$ *GUT with* $\sin^2(\theta_W^0) = 3/8$, *Phys. Lett.* **B 564** (2003) 35 [hep-th/0301177] [INSPIRE].

[8] S. Willenbrock, *Triplicated trinification*, *Phys. Lett.* **B 561** (2003) 130 [hep-ph/0302168] [INSPIRE].

[9] C.D. Carone and J.M. Conroy, *Higgsless GUT breaking and trinification*, *Phys. Rev.* **D 70** (2004) 075013 [hep-ph/0407116] [INSPIRE].

[10] J. Hetzel, *Phenomenology of a left-right-symmetric model inspired by the trinification model*, arXiv:1504.06739 [INSPIRE].

[11] F. Gursey, P. Ramond and P. Sikivie, *A universal gauge theory model based on* E_6, *Phys. Lett.* **B 60** (1976) 177 [INSPIRE].

[12] Y. Achiman and B. Stech, *Quark lepton symmetry and mass scales in an* E_6 *unified gauge model*, *Phys. Lett.* **B 77** (1978) 389 [INSPIRE].

[13] Q. Shafi, E_6 *as a unifying gauge symmetry*, *Phys. Lett.* **B 79** (1978) 301 [INSPIRE].

[14] R. Barbieri, D.V. Nanopoulos and A. Masiero, *Hierarchical fermion masses in* E_6, *Phys. Lett.* **B 104** (1981) 194 [INSPIRE].

[15] B. Stech and Z. Tavartkiladze, *Fermion masses and coupling unification in* E_6*: life in the desert*, *Phys. Rev.* **D 70** (2004) 035002 [hep-ph/0311161] [INSPIRE].

[16] B. Stech, *Neutrino properties from* $E_6 \times \mathrm{SO}(3) \times Z_2$, *Fortsch. Phys.* **58** (2010) 692 [arXiv:1003.0581] [INSPIRE].

[17] S.F. King, S. Moretti and R. Nevzorov, *Exceptional supersymmetric Standard Model*, *Phys. Lett.* **B 634** (2006) 278 [hep-ph/0511256] [INSPIRE].

[18] S.F. King, S. Moretti and R. Nevzorov, *Theory and phenomenology of an exceptional supersymmetric Standard Model*, *Phys. Rev.* **D 73** (2006) 035009 [hep-ph/0510419] [INSPIRE].

[19] S.F. King, S. Moretti and R. Nevzorov, *Gauge coupling unification in the exceptional supersymmetric Standard Model*, *Phys. Lett.* **B 650** (2007) 57 [hep-ph/0701064] [INSPIRE].

[20] F. Braam, A. Knochel and J. Reuter, *An exceptional SSM from* E_6 *orbifold GUTs with intermediate LR symmetry*, *JHEP* **06** (2010) 013 [arXiv:1001.4074] [INSPIRE].

[21] P. Athron et al., *The constrained* E_6*SSM*, arXiv:0810.0617 [INSPIRE].

[22] S.F. King, R. Luo, D.J. Miller and R. Nevzorov, *Leptogenesis in the exceptional supersymmetric Standard Model: flavour dependent lepton asymmetries*, *JHEP* **12** (2008) 042 [arXiv:0806.0330] [INSPIRE].

[23] P. Athron, S.F. King, D.J. Miller, S. Moretti and R. Nevzorov, *Predictions of the constrained exceptional supersymmetric Standard Model*, *Phys. Lett.* **B 681** (2009) 448 [arXiv:0901.1192] [INSPIRE].

[24] P. Athron, S.F. King, D.J. Miller, S. Moretti and R. Nevzorov, *The constrained exceptional supersymmetric Standard Model*, *Phys. Rev.* **D 80** (2009) 035009 [arXiv:0904.2169] [INSPIRE].

JHEP09(2016)129

[25] P. Athron, S.F. King, D.J. Miller, S. Moretti and R. Nevzorov, *LHC signatures of the constrained exceptional supersymmetric Standard Model*, *Phys. Rev.* **D 84** (2011) 055006 [arXiv:1102.4363] [INSPIRE].

[26] J.P. Hall et al., *Novel Higgs decays and dark matter in the E_6SSM*, *Phys. Rev.* **D 83** (2011) 075013 [arXiv:1012.5114] [INSPIRE].

[27] P. Athron, S.F. King, D.J. Miller, S. Moretti and R. Nevzorov, *Constrained exceptional supersymmetric Standard Model with a Higgs near* 125 *GeV*, *Phys. Rev.* **D 86** (2012) 095003 [arXiv:1206.5028] [INSPIRE].

[28] R. Nevzorov, *E_6 inspired supersymmetric models with exact custodial symmetry*, *Phys. Rev.* **D 87** (2013) 015029 [arXiv:1205.5967] [INSPIRE].

[29] R. Nevzorov and S. Pakvasa, *Exotic Higgs decays in the E_6 inspired SUSY models*, *Phys. Lett.* **B 728** (2014) 210 [arXiv:1308.1021] [INSPIRE].

[30] R. Nevzorov, *Quasifixed point scenarios and the Higgs mass in the E_6 inspired supersymmetric models*, *Phys. Rev.* **D 89** (2014) 055010 [arXiv:1309.4738] [INSPIRE].

[31] R. Nevzorov and A.W. Thomas, *E_6 inspired composite Higgs model*, *Phys. Rev.* **D 92** (2015) 075007 [arXiv:1507.02101] [INSPIRE].

[32] P. Athron, D. Harries, R. Nevzorov and A.G. Williams, *E_6 inspired SUSY benchmarks, dark matter relic density and a* 125 *GeV Higgs*, *Phys. Lett.* **B 760** (2016) 19 [arXiv:1512.07040] [INSPIRE].

[33] S.F. King and R. Nevzorov, 750 *GeV diphoton resonance from singlets in an exceptional supersymmetric Standard Model*, *JHEP* **03** (2016) 139 [arXiv:1601.07242] [INSPIRE].

[34] P. Athron, D. Stöckinger and A. Voigt, *Threshold corrections in the exceptional supersymmetric Standard Model*, *Phys. Rev.* **D 86** (2012) 095012 [arXiv:1209.1470] [INSPIRE].

[35] Y. Kawamura and T. Miura, *Classification of Standard Model particles in E_6 orbifold grand unified theories*, *Int. J. Mod. Phys.* **A 28** (2013) 1350055 [arXiv:1301.7469] [INSPIRE].

[36] T.G. Rizzo, *Gauge kinetic mixing in the E_6SSM*, *Phys. Rev.* **D 85** (2012) 055010 [arXiv:1201.2898] [INSPIRE].

[37] J. Reuter and D. Wiesler, *Distorted mass edges at LHC from supersymmetric leptoquarks*, *Phys. Rev.* **D 84** (2011) 015012 [arXiv:1010.4215] [INSPIRE].

[38] D.J. Gross, J.A. Harvey, E.J. Martinec and R. Rohm, *The heterotic string*, *Phys. Rev. Lett.* **54** (1985) 502 [INSPIRE].

[39] E. Cremmer, J. Scherk and J.H. Schwarz, *Spontaneously broken $N = 8$ supergravity*, *Phys. Lett.* **B 84** (1979) 83 [INSPIRE].

[40] E. Ma, *Particle dichotomy and left-right decomposition of E_6 superstring models*, *Phys. Rev.* **D 36** (1987) 274 [INSPIRE].

[41] E. Ma, *Neutrino masses in an extended gauge model with E_6 particle content*, *Phys. Lett.* **B 380** (1996) 286 [hep-ph/9507348] [INSPIRE].

[42] J.E. Kim, *Trinification with $\sin^2\theta_W = 3/8$ and seesaw neutrino mass*, *Phys. Lett.* **B 591** (2004) 119 [hep-ph/0403196] [INSPIRE].

JHEP09(2016)129

[43] C. Cauet, H. Pas, S. Wiesenfeldt, H. Pas and S. Wiesenfeldt, *Trinification, the hierarchy problem and inverse seesaw neutrino masses*, *Phys. Rev.* **D 83** (2011) 093008 [arXiv:1012.4083] [INSPIRE].

[44] J. Sayre, S. Wiesenfeldt and S. Willenbrock, *Minimal trinification*, *Phys. Rev.* **D 73** (2006) 035013 [hep-ph/0601040] [INSPIRE].

[45] C.-S. Huang, J. Jiang, T.-J. Li and W. Liao, $N = 2$ *six-dimensional supersymmetric* E_6 *breaking*, *Phys. Lett.* **B 530** (2002) 218 [hep-th/0112046] [INSPIRE].

[46] H. Georgi, *Towards a grand unified theory of flavor*, *Nucl. Phys.* **B 156** (1979) 126 [INSPIRE].

[47] B. Stech, *Trinification phenomenology and the structure of Higgs bosons*, *JHEP* **08** (2014) 139 [arXiv:1403.2714] [INSPIRE].

[48] J. Hetzel and B. Stech, *Low-energy phenomenology of trinification: an effective left-right-symmetric model*, *Phys. Rev.* **D 91** (2015) 055026 [arXiv:1502.00919] [INSPIRE].

[49] T. Lee, T. Li and C. Tsai, *Hom4PS-2.0: a software package for solving polynomial systems by the polyhedral homotopy continuation method*, *Computing* **83** (2008) 109.

[50] C.P. Burgess, *A Goldstone boson primer*, in 11th *Summer School and Symposium on Nuclear Physics (NuSS 98): Effective Theories of Matter*, Seoul South Korea June 23–27 1998 [hep-ph/9812468] [INSPIRE].

[51] C.P. Burgess, *Goldstone and pseudo-Goldstone bosons in nuclear, particle and condensed matter physics*, *Phys. Rept.* **330** (2000) 193 [hep-th/9808176] [INSPIRE].

[52] A. Dedes, A.B. Lahanas and K. Tamvakis, *Radiative electroweak symmetry breaking in the MSSM and low-energy threshold*, *Phys. Rev.* **D 53** (1996) 3793 [hep-ph/9504239] [INSPIRE].

[53] G. Gamberini, G. Ridolfi and F. Zwirner, *On radiative gauge symmetry breaking in the minimal supersymmetric model*, *Nucl. Phys.* **B 331** (1990) 331 [INSPIRE].

[54] M. Carena, S. Pokorski and C.E.M. Wagner, *On the unification of couplings in the minimal supersymmetric Standard Model*, *Nucl. Phys.* **B 406** (1993) 59 [hep-ph/9303202] [INSPIRE].

[55] ATLAS collaboration, *Search for new resonances in events with one lepton and missing transverse momentum in pp collisions at* $\sqrt{s} = 13$ *TeV with the ATLAS detector*, arXiv:1606.03977 [INSPIRE].

[56] ATLAS collaboration, *Search for new phenomena in the dilepton final state using proton-proton collisions at* $\sqrt{s} = 13$ *TeV with the ATLAS detector*, ATLAS-CONF-2015-070, CERN, Geneva Switzerland (2015).

[57] F. Lyonnet, I. Schienbein, F. Staub and A. Wingerter, *PyR@TE: renormalization group equations for general gauge theories*, *Comput. Phys. Commun.* **185** (2014) 1130 [arXiv:1309.7030] [INSPIRE].

[58] S. Kirkpatrick, C.D. Gelatt and M.P. Vecchi, *Optimization by simulated annealing*, *Science* **220** (1983) 671 [INSPIRE].

JHEP09(2016)129